NAS CR 135135
PWA-5471

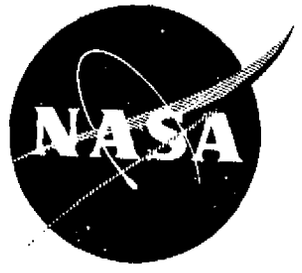

ANALYSIS AND DESIGN OF DIGITAL OUTPUT INTERFACE DEVICES FOR GAS TURBINE ELECTRONIC CONTROLS FINAL REPORT

by

D. M. Newirth
E. W. Koenig

PRATT & WHITNEY AIRCRAFT DIVISION
UNITED TECHNOLOGIES CORPORATION

December 1976

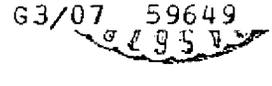

prepared for

NATIONAL AERONAUTICS AND SPACE ADMINISTRATION
NASA LEWIS RESEARCH CENTER
CONTRACT NAS3-19898

1. Report No.	2. Government Accession No.	3. Recipient's Catalog No.
CR 135135		

4. Title and Subtitle	5. Report Date
Analysis and Design of Digital Output Interface Devices for Gas Turbine Electronic Controls – Final Report	December 1976
	6. Performing Organization Code
7. Author(s)	8. Performing Organization Report No.
D. M. Newirth E. W. Koenig	PWA-5471
	10. Work Unit No.
9. Performing Organization Name and Address	11. Contract or Grant No.
Pratt & Whitney Aircraft Division United Technologies Corporation East Hartford, Conn. 06108	NAS3-19898
	13. Type of Report and Period Covered
12. Sponsoring Agency Name and Address	Contractor Report
NASA-Lewis Research Center Cleveland, Ohio 44135	14. Sponsoring Agency Code

15. Supplementary Notes

Project Monitor, Leon M. Wenzel
Wind Tunnell and Flight Division,
NASA – Lewis Research Center, Cleveland, Ohio

Final Report

16. Abstract

A trade study was performed on twenty-one digital output interface schemes for gas turbine electronic controls to select the most promising scheme based on criteria of reliability, performance, cost, and sampling requirements. The most promising scheme, a digital effector with optical feedback of the fuel metering valve position, was designed.

17. Key Words (Suggested by Author(s))	18. Distribution Statement
Digital Output Interface Devices Digital Electronic Controls Output Devices – Electronic Controls Optical Position Transducer	Unclassified – Unlimited

19. Security Classif. (of this report)	20. Security Classif. (of this page)	21. No. of Pages	22. Price*
Unclassified	Unclassified	66	

* For sale by the National Technical Information Service, Springfield, Virginia 22151

NASA-C-168 (Rev. 6-71)

TABLE OF CONTENTS

Section	Subject	Page
I.	Summary	1
II.	Introduction	3
III.	Digital Output Interface (DOI) Scheme Trade Study	4
	A. Trade Study Criteria	5
	B. Selection of DOI Schemes for Trade Study	5
	C. Component Data	7
	D. DOI Scheme Simulations	7
	E. Reliability Analysis	8
	F. Life Cycle Cost Analysis	8
	G. Performance Analysis and Evaluation	9
	1. Transient Response	10
	2. Steady-State Accuracy: Closed-Loop Control	10
	3. Steady-State Accuracy: Open-Loop Control	11
	4. Steady-State Stability	11
	5. Results of Performance Evaluation	12
	H. Failure Modes and Effects Analysis	12
	I. Final Evaluation	13
	J. Trade Study Conclusions and Recommendations	14
IV.	Design of the Selected DOI Scheme	15
	A. Digital Effector Design	15
	1. Solenoid Valve Selection	15
	2. Solenoid Configuration	15
	B. Optical Position Sensor	18
	C. Hydrochemical Fuel Flow Test Package	19
	1. Fuel Metering Valve	19
	2. Minimum Pressurizing Valve	21
	3. Filter and Relief Valve	21
	4. Position Sensor	22
	D. Interfacing Electronics	22
	1. Solenoid Drive Circuits	22
	2. Optic-Electronic Interface	22
	3. Resolver-to-Digital Converter	25
	4. Serial Data Transmission	25
	5. Interconnecting Cabling	25
	E. Software Logic for the Electronic Controller	25
	1. Dynamic Simulation	25
	2. Adaptive Logic	27

TABLE OF CONTENTS (Cont'd)

Section	Subject	Page
	F. Dynamic Analysis of Proposed Designs	31
	1. Dynamic Analysis of Preliminary Designs	31
	a. Digital Effector: Two-Solenoid Configuration	31
	b. Optical Encoder Linkage Loading	31
	c. Optical Position Feedback Resolution	31
	d. Failure Analysis of the Two-Solenoid Configuration	36
	2. Review of Final Designs	36
	a. Digital Effector: Four-Solenoid Configuration	36
	b. Optical Encoder Linkage Loading	36
	c. Failure Analysis of the Four-Solenoid Configuration	39
V.	Conclusions	41
Appendix A	Block Diagrams of DOI Schemes	55
Appendix B	Calculation of Adaptive Gain	59

LIST OF TABLES

Table	Title	Page
1	Digital Output Interface Devices Component Data	42
2	Reliability of the Digital Output Interface Schemes	43
3	Cost, Weight, Maintenance and Life Cycle Cost of the Digital Output Interface Schemes	44
4	Performance Evaluation of the Digital Output Interface Schemes	45
5	Sampling Time Limitations	46
6	Performance Evaluation of the Most Promising Digital Output Interface Schemes at Sea Level Static	47
7	Performance Evaluation of the Most Promising Digital Output Interface Schemes at Altitude Cruise	48
8	Final Performance Evaluation of the Most Promising Digital Output Interface Schemes	49
9	Sampling Interval Time Evaluation of the Most Promising Digital Output Interface Schemes	50
10	Final Evaluation of the Most Promising Digital Output Interface Schemes	51
11	Comparison of Gray and Binary Codes	52
12	Solenoid Failure Consequences: Two-Solenoid Scheme	53
13	Solenoid Failure Consequences: Four-Solenoid Scheme	54

LIST OF ILLUSTRATIONS

Figure	Title	Page
1	Digital Output Interface	1
2	Digital Output Interface Trade Study Procedure	4
3	Engine/Controller Configuration Used for the Performance Evaluation of the Digital Output Interface Schemes	6
4	Controller and Digital Output Interface Transfer Function	6
5	Timing Diagram for DOI Simulation	8
6	Two-Solenoid Configuration	16
7	Three-Solenoid Configuration	17
8	Four-Solenoid Configuration	18
9	Schematic of Optical Position Sensor	20
10	Schematic of Fuel Flow Package	20
11	Fuel Flow Package Including the Solenoid Actuators and the Optical Position Sensor	21
12	Simplified Schematic of Light-Emitting Diode (LED) Drive Circuit	23
13	Optical Position Sensor Receiver Circuit	24
14	Block Diagram of Digital Effector and Metering Valve Actuator	26
15	Electronic Control Software Schematic	28
16	Block Diagram of the Adaptive Logic	29
17	Metering Valve Position Control Loop	29
18	Small Power Lever Step and Steady-State Operation at Sea Level Static, High Power with the Two-Solenoid Configuration and with Revised Adapative Logic	30
19	Small Power Lever Step and Steady-State Operation at Sea Level Static, High Power with the Two-Solenoid Configuration without Adaptive Logic	32

LIST OF ILLUSTRATONS (Cont'd)

Figure	Title	Page
20	Response of the Two-Solenoid Digital Effector with 12-bit Position Feedback Resolution to Small Power Lever Step at Sea Level Static, High Power	33
21	Steady-State Cycling at Idle Due to Optical Encoder Linkage Loading	34
22	Response of Two-Solenoid Configuration with the Original Adaptive Logic and .002 Inch Position Feedback Resolution to a Small Power Lever Step at Sea Level Static, High Power	35
23	Small Power Lever Step and Steady-State Operation at Sea Level Static, High Power with the Four-Solenoid Configuration	37
24	Small Power Lever Step and Steady State Operation at Idle with the Four-Solenoid Configuration and with Reduced Loading from the Optical Encoder	38
25	Response Due to One Increase Solenoid Failing Open at Sea Level Static, High Power	40

I. SUMMARY

The initial objective of the digital output interface (DOI) program was to select a high technology, innovative digital electronic control output device which has the potential for high reliability and low-cost maintainability in an aircraft gas turbine digital electronic propulsion control. This selection was accomplished through a trade study in which twenty-one proposed DOI schemes were evaluated to select the one which showed the most promise in terms of reliability, performance and cost. A DOI is defined as that portion of a digital electronic control which converts a digital word into a mechanical position, and consists of a combination of electronic, electro-mechanical and mechanical components (Figure 1). For this study, each DOI scheme was configured to control fuel flow as a subsystem of a closed loop digital electronic gas turbine controller.

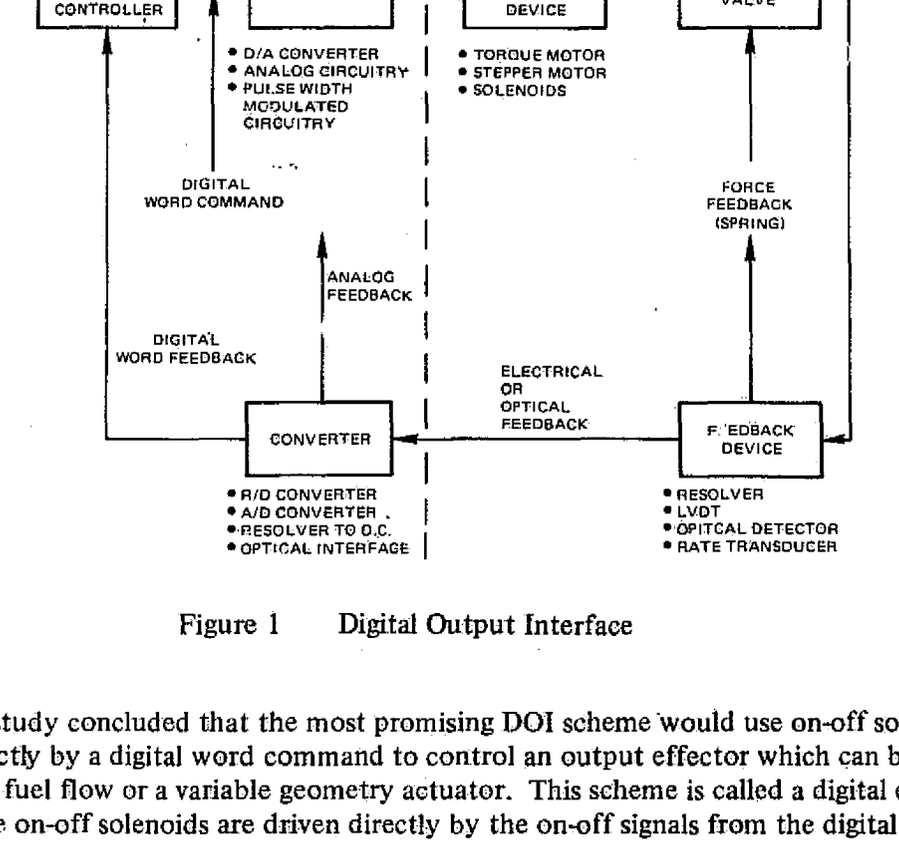

Figure 1 Digital Output Interface

The trade study concluded that the most promising DOI scheme would use on-off solenoids driven directly by a digital word command to control an output effector which can be used to regulate fuel flow or a variable geometry actuator. This scheme is called a digital effector because the on-off solenoids are driven directly by the on-off signals from the digital electronic controller. Each solenoid in turn regulates the servo actuating flow in a hydromechanical control to position a fuel metering valve or other mechanical actuator. (The digital effector is the subject of a U. S. patent application, Adaptive Control System Using Position Feedback filed on June 11, 1975, U. S. Serial Number 586010, by Anthony N. Martin, and assigned to United Technologies Corporation.)

The trade study indicated that torque motor and stepper motor DOI schemes could also provide adequate fuel flow control, but would be more expensive and less reliable than a digital effector. The main advantage of the digital effector is its simplicity; the only components are the solenoids and simple drive circuitry. (The drive circuitry allows the digital word command, which is a low DC voltage, to trigger the solenoids through a 28 volt DC power source.) Torque motors and stepper motors are inherently more expensive and less reliable than on-off solenoids and require more complex conversion and drive circuitry.

An optical position sensor was selected to provide fuel valve position feedback. The sensor consists of a light-emitting diode and its drive circuit, a fiber optic cable system, a Gray code encoder plate, and an eight-channel light-sensitive receiver circuit. The optical sensor was selected based on predicted reliability and cost advantages over more conventional position sensors, such as a potentiometer, resolver or a linear variable differential transformer (LVDT). These conventional sensors would require an analog-to-digital (A/D) converter or a resolver-to-digital (R/D) converter to convert a D.C. voltage or sinusoidal phase angle to a digital word. An optical sensor has a much simpler interface because each of the eight receiver channels is directly converted to one bit of the eight-bit digital word. The optical signal from each individual channel is converted directly to an "on" signal (high voltage corresponding to a "one" bit in the software) or an "off" (low voltage or "zero" bit) signal depending on whether the light sensitivity exceeds the reference threshold level.

The software of the selected DOI scheme uses adaptive logic to control system response. The adaptive logic estimates hardware characteristics based on measurements of the fuel valve position. This estimate is used to vary a software gain to effect a desired gain and response of the DOI system.

It was concluded that a digital effector with optical position feedback and adaptive logic in the software has potential reliability and cost advantages over more conventional digital output interface (DOI) approaches. Therefore the preliminary and final design tasks of this contract were performed on a prototype version of this device for the control of a fuel metering valve in a gas turbine full authority electronic control.

II. INTRODUCTION

Recent studies at Pratt & Whitney Aircraft have indicated that considerable savings, in both maintenance expense and life cycle cost, can be realized by using digital electronic controllers for gas turbine engines. Automatic troubleshooting, self test devices, and less costly maintenance materials result in lower maintenance costs compared to current all-hydromechanical controls. This lower maintenance cost coupled with the lower procurement cost of electronic controls results in a lower predicted life cycle cost. Also, the ease with which redundancy can be achieved in electronic systems should all but eliminate total control system failures and in-flight shutdowns, and will generally enhance overall control system reliability. But while redundancy improves system mission reliability, it also adds complexity, with attendant maintenance, weight, and cost penalties. To minimize these penalties, the major thrust of electronic control system development must be to achieve maximum reliability and maintainability at the component and subsystem level.

In determining which components will provide the greatest potential for improvement in system reliability, a digital electronic control was divided into four major subsystems: power supply, input and output interface, digital processor, and memory. It has been estimated that the input and output interface subsystem contributes approximately one-half of the total weight and seventy percent of the total failures of a typical digital electronic control for a commercial turbofan engine. For this reason, Pratt & Whitney Aircraft feels that substantial improvements in the interface portion of digital electronic control systems will be required to help insure that maximum reliability and maintainability can be achieved.

Under NASA Contract NAS3-19898, Pratt & Whitney Aircraft conducted a program to improve the reliability of digital output interface (DOI) subsystems in digital electronic controls. A DOI is defined as the subsystem of a digital electronic control which converts a digital word into a mechanical position. The program was conducted in three tasks:

- Task 1, a trade study which considered many different DOI schemes and identified the best scheme. (A DOI scheme is defined as the combination of components in a DOI, such as a torque motor with an integrator and a feedback device.)
- Task 2, preliminary design, where several design concepts for the selected DOI scheme were considered.
- Task 3, final design of a prototype DOI.

In order to evaluate the merits of various methods for converting from a digital word command to a mechanical position, a comprehensive trade study was devised. The trade study considered reliability/maintainability factors, performance factors such as accuracy and response, digital sampling requirements, cost, and weight. The details of this study are discussed in Section III. The DOI scheme identified as best was further developed by performing preliminary designs and a final prototype design. This work is described in Section IV of the report.

III. DOI SCHEME TRADE STUDY

A comprehensive trade study was conducted in which twenty-one promising DOI schemes were evaluated to select the most promising one based on the criteria of reliability, performance, cost, and sampling requirements. The trade study procedure is diagrammed in Figure 2.

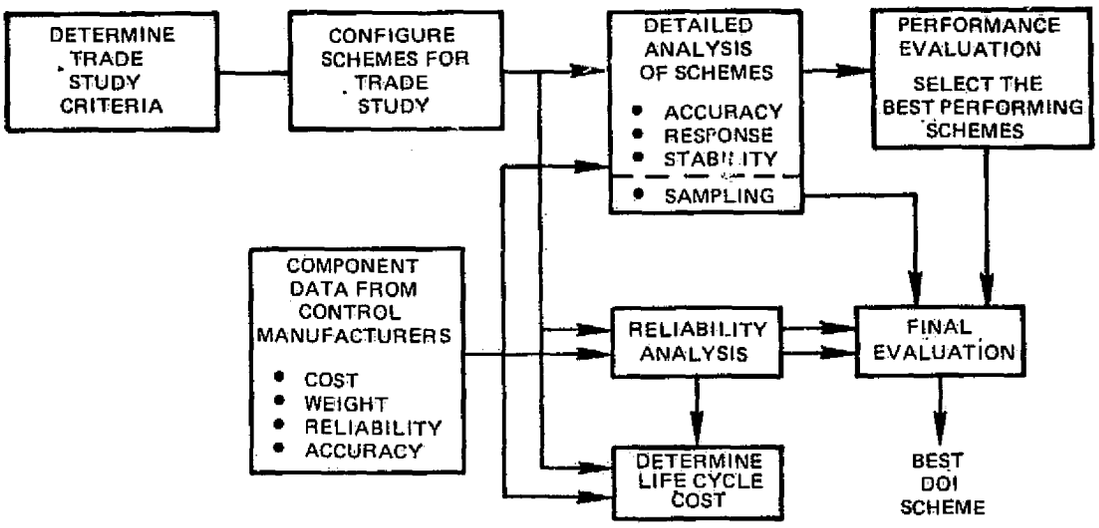

Figure 2 Digital Output Interface Trade Study Procedure

Sixty-seven DOI schemes were initially configured by considering every possible combination of DOI components. This was narrowed down to twenty-one schemes for the trade study by eliminating non-integrating or multiple-integrating schemes.

Pratt & Whitney Aircraft selected two control manufacturers, Hamilton Standard and Bendix to contribute interface suggestions and to supply cost, weight, reliability, and accuracy data for DOI components under consideration for the schemes in the trade study. Component data was obtained from the two manufacturers so the trade study would not be unfairly biased for or against any particular DOI schemes or components.

Cost, weight, and reliability data supplied by the control manufacturers were used to calculate the reliability and life cycle cost of each scheme. The performance of the twenty-one DOI schemes was evaluated based on transient response, steady-state accuracy, and steady-state stability. The best performing DOI schemes were compared in a final evaluation which identified the best scheme based on reliability, life cycle cost, performance, and sampling requirements.

A. TRADE STUDY CRITERIA

In order for a DOI scheme to become a viable candidate for incorporation in a digital electronic control system, it must have two major attributes: acceptable performance in terms of accuracy and response, and reliability. One attribute present without the other in a candidate DOI scheme makes it unsuitable for gas turbine control systems. Cost based on the entire life cycle was also considered in the trade study. To summarize, each candidate DOI scheme was evaluated on the following criteria:

- Reliability
- Performance
- Life cycle cost
- Sampling requirements

Weighting factors were chosen to give a relative level of importance to the four categories. Reliability and performance were weighted the highest, life cycle cost slightly less, and sampling requirements the least important.

B. SELECTION OF DOI SCHEMES FOR THE TRADE STUDY

Sixty-seven DOI schemes were initially configured by tabulating every possible combination of components. For example, a DOI scheme could use a torque motor, a stepper motor, or solenoids; the integrator could be located in the digital electronics, the analog interface electronics, or in the hydromechanical unit. A scheme could use position feedback, rate feedback, or no feedback, and the feedback could be either hydromechanical, digital electronic, or analog electronic. A resolver, a linear variable differential transformer (LVDT), or an optical position sensor could be used as the feedback device. Some DOI schemes were eliminated because they were not integrating controls, other schemes were eliminated because of multiple integrations. This narrowed the selection down to the twenty-one schemes shown in the block diagrams of Appendix A. Schemes with position feedback were expanded into two or three sub-schemes: a resolver with a resolver-to-digital or a resolver-to-D.C. converter, an LVDT with an analog-to-digital converter, and also an optical sensor and interface for those schemes with position feedback to the digital electronics.

The trade study included several simple schemes with hydromechanical feedback or no feedback. It was anticipated that these schemes would rank low in the performance evaluation but would have reliability and cost advantages over the more complicated schemes.

Each of the twenty-one DOI schemes was evaluated as part of a closed loop electronic control (Figure 3) operating a high bypass ratio turbofan engine. Dynamic compensation in the controller and the transfer functions of all DOI schemes were designed to be as functionally equivalent as possible (Figure 4).

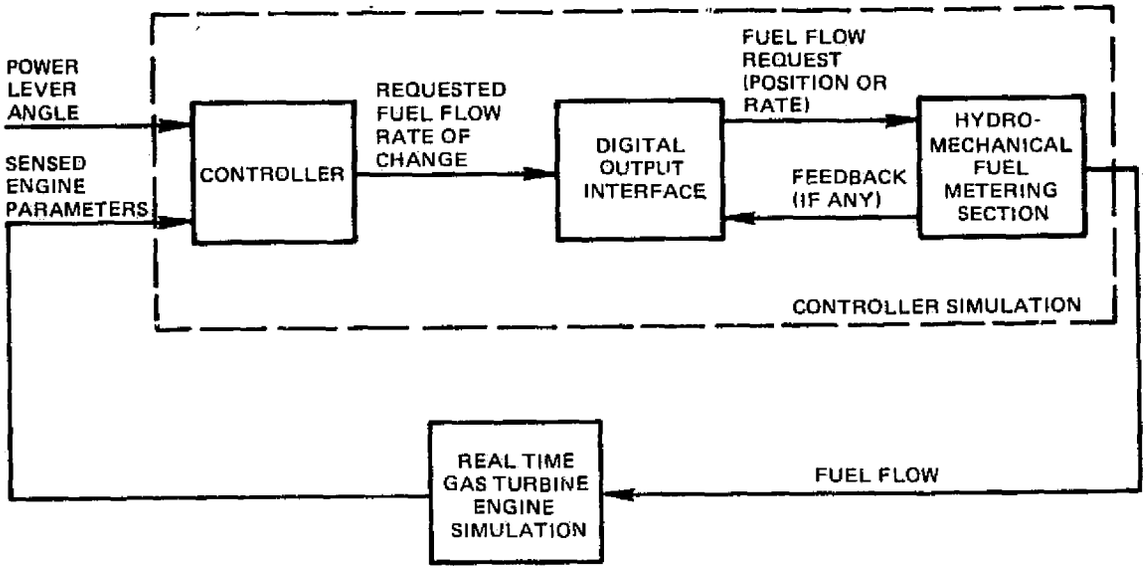

Figure 3 Engine/Controller Configuration Used for the Performance Evaluation of the Digital Output Interface Schemes

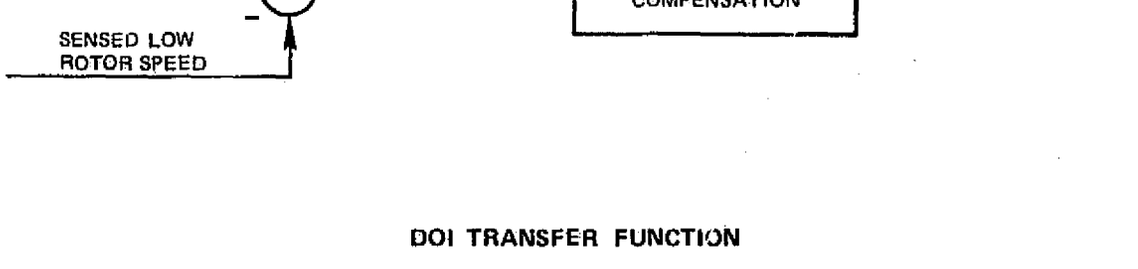

DOI TRANSFER FUNCTION

$$\frac{\text{FUEL FLOW (S)}}{\text{REQUESTED FUEL FLOW RATE OF CHANGE (S)}} = \frac{1}{S(.02S + 1)} \quad \text{(FOR SCHEMES WITH FEEDBACK)}$$

$$\frac{1}{S} \quad \text{(FOR SCHEMES WITHOUT FEEDBACK)}$$

Figure 4 Controller and Digital Output Interface Transfer Function

C. COMPONENT DATA

Two control manufacturers, Hamilton Standard and Bendix, supplied cost, weight, reliability, and accuracy data for the DOI components (torque motors, stepper motors, solenoids, digital-to-analog converters, etc.) of the twenty-one schemes in the trade study. When the manufacturers submitted different data for the same component, Pratt & Whitney Aircraft contacted the manufacturers to verify that the components were comparable. When the data was for different component devices (i.e., a #18 stepper motor versus a #11 stepper motor), Pratt & Whitney Aircraft selected the device it felt was best suited for interfacing with a gas turbine fuel flow control. When the data was different for the same component device, Pratt & Whitney Aircraft investigated both manufacturers' source of the quoted data and made a judgment on which data to use, or averaged the data if the differences were small. The component data used for the trade study is tabulated in Table 1.

All of the components except the optical sensor and interface have been used by Hamilton and Bendix in recent propulsion control programs. Estimates for the optical components are based on piece part breakdowns applied to the production version of an optical sensor and interface being developed by United Technologies Research Center. Cost figures are off the shelf prices in 1975 dollars for moderate production quantity and do not include any engineering labor or development cost. The accuracy data tabulated is for the specific component devices selected for the DOI schemes in the trade study and represents the projected state-of-the-art for engine-mounted flightworthy components. The reliability data is based on components in an engine-mounted electronic control operating at an ambient temperature of 394°K [250°F] and a fuel cooling temperature of 372°K [210°F]. The reliability figures are based on the control manufacturer's experience from recent propulsion control programs or data from reliability handbooks (Rome Air Data Center [RADC] Handbook, Volume 2; Mil Handbook 217B, Reliability Prediction of Electronic Equipment, and Failure Rate Data [FARADA] Handbooks) where data from the handbooks is more appropriate due to limited operational experience with the specific component under consideration.

D. DOI SCHEME SIMULATIONS

A digital computer simulation of each DOI scheme was developed to evaluate performance and to determine sampling requirements. Each DOI scheme was simulated as a separate computer subroutine. The DOI scheme simulations were operated with simulations of a digital electronic controller, a hydromechanical fuel control, and a transfer function simulation of a high bypass ratio turbofan engine. The engine, hydromechanical control, and the continuous portion of each DOI scheme (analog electronics, torque motor and driver, stepper motor position, fuel valve, LVDT, resolver) were simulated with a computing time interval (DT) of 5 milliseconds. The sampling time of the digital electronic controller was a variable input, its only restriction being that it must be an integral multiple of 5 milliseconds. Update times of the engine parameters and control parameters measured by the digital electronic controller (rotor speed, fuel valve position) were also variable, as were delay times from each parameter update to the digital-to-analog (D/A) converter. A timing diagram of the digital electronic controller used for the DOI simulations is shown in Figure 5.

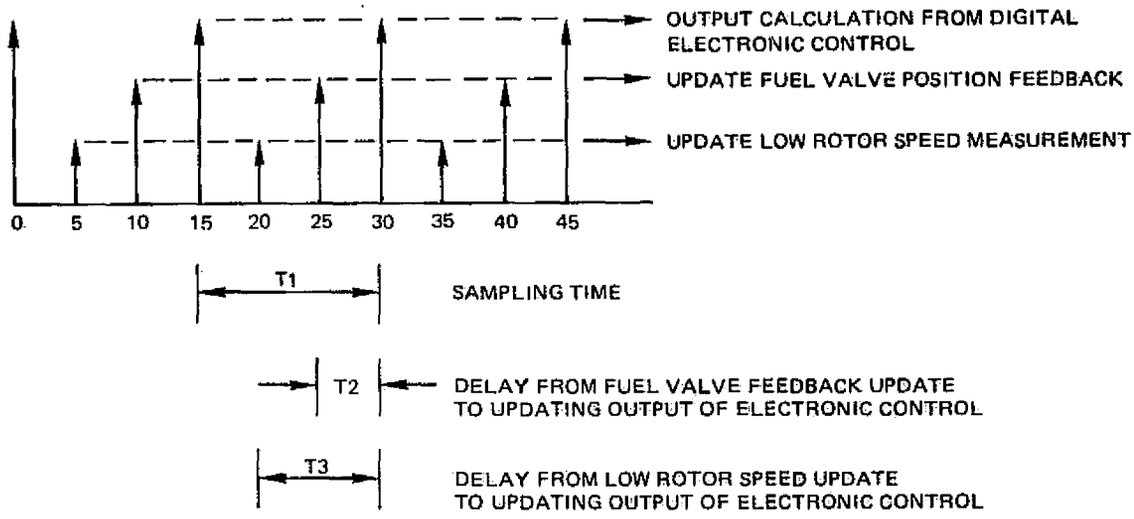

Figure 5 Timing Diagram for D.O.I. Simulations

Data output consisted of off-line printouts in column form, each column containing fifty variables for a single point in time. Output variables were time, flight condition, power lever angle, engine parameters, fuel valve position and engine fuel flow, servo flow, DOI parameters such as D/A voltage, torque motor current, stepper motor position, solenoid on-time and various parameters inside the digital electronic controller. Graphics output included "rough" on-line plots from the computer terminals, and higher quality off-line plots.

E. RELIABILITY ANALYSIS

A reliability analysis was performed on the twenty-one DOI schemes. Parts count and operational reliability were calculated using the component data in Table 1. The failure rates of all DOI components in each scheme (excluding the software in the electronic controller) were totalled together to determine the parts count reliability, expressed in units of failures per million hours. Operational reliability was determined by totalling the failure rates of only those DOI components whose failure would cause a system failure. The parts count reliability and the operational reliability of the DOI schemes are tabulated in Table 2.

Based on the component data listed in Table 1, DOI schemes with solenoids (Schemes 16-21) would have lower failure rates than schemes which included a torque motor (Schemes 1-9) or a stepper motor (Schemes 10-15).

F. LIFE CYCLE COST ANALYSIS

A life cycle cost study was performed on the twenty-one DOI schemes to determine the impact of operating electronic controls with each of the schemes in commercial service over an assumed useful life of 50,000 hours. Cost, weight, and reliability data supplied by the control

manufacturers (Table 1) were used to calculate the life cycle cost. The life cycle cost is the sum of the initial cost plus the cost of spares, the cost to fly the weight of each scheme for 50,000 hours, plus maintenance material and labor. The initial cost is the sum cost of the individual components, plus an assumed 25% spare control requirement. The weight cost is the fuel cost per gross weight, assuming a 4828 kilometer (3000 mile) mission at an average speed of 257 meters per second (575 miles per hour) with the price of JP4 at 5.19¢ per liter (22.86¢ per gallon). Maintenance material cost is the piece-part replacement cost times the component failure rate. Maintenance labor cost is the average cost to repair a failure, based on a labor rate of $12.50 per hour, times the DOI scheme failure rate. The life cycle cost of the twenty-one DOI schemes is tabulated in Table 3.

Reliability has a strong effect on the life cycle cost, therefore, the life cycle cost ranking followed the same trend as the reliability ranking: solenoid schemes would have a lower life cycle cost than torque motor or stepper motor schemes.

G. PERFORMANCE ANALYSIS AND EVALUATION

The performance of the twenty-one DOI schemes was analyzed and evaluated based on the following criteria:

- Transient response at high power
- Steady-state accuracy: closed loop control
- Steady-state accuracy: open loop control
- Steady-state stability

Component accuracy data from the control manufacturers and fuel valve noise characteristics recorded during digital electronic control engine testing were input to the DOI simulations. The simulations were exercised to determine response, accuracy and stability.

During the performance evaluation, it became evident that DOI Scheme 17 is not a feasible configuration. The on-off solenoid signals cannot be made equivalent to a modulated position request because the solenoid signals have only three states: increase solenoid energized, both solenoids de-energized, and decrease solenoid energized. Trying to schedule a position with this configuration would subject the fuel valve to extreme oscillations or would require solenoids with large dynamic lag making transient response unacceptable. Therefore, Scheme 17 was eliminated from further consideration.

The DOI schemes were ranked from 1 to 4, with 1 being the best in each of the four performance categories. If a scheme exhibited performance far worse than the other schemes, it was ranked 4+ and the data for the other schemes was used to determine the rankings for that particular performance category.

Weighting factors were assigned to each performance category. The rankings for each performance category were multiplied by the appropriate weighting factor and then added together to determine the total performance ranking for each DOI scheme. Steady-state accuracy for closed loop control and open loop control, and steady-state stability had weighting factors of two. Transient response was weighted only one because the software gains and compensation were not optimized for each scheme.

The results of the performance evaluation are tabulated in Table 4.

1. Transient Response

The transient response is defined as the time for 90% of the requested low rotor speed change for a small power lever step at high power. The range of response time reflects variations in component accuracy, gain, hysteresis, resolution and noise. Response time was determined by running the computer simulation with nominal DOI components, and then including typical component variations, one at a time, to determine the change in response time. The changes in response time for the component variations were root-sum-squared to determine the range of response time for each DOI scheme.

The transient response ranking reflected variation in response because the nominal response is controllable through software optimization; the variation in response is characteristic of each scheme and its particular components. Response would vary randomly from unit-to-unit within the limits determined during the performance evaluation.

Torque motor schemes consistently showed a moderate variation in transient response time. Some stepper motor schemes had very little variation in response, while others showed very large variations. Solenoid schemes exhibited a trend similar to the stepper motor schemes.

2. Steady-State Accuracy: Closed Loop Control

Steady-state accuracy for closed loop control is defined as the accuracy of controlling the engine low rotor speed. The speed error, which is defined as the difference between the requested and measured speed, was calculated for typical errors of each DOI component. (Errors in the speed measurement were not included because the speed measurement is not a part of the digital output interface.) The individual speed errors were root-sum-squared to determine the steady-state speed error of each DOI scheme.

The following general observations were made about closed-loop control accuracy:

- Schemes with a digital integrator and position feedback (Schemes 1, 2, 3, 10, and 16) would provide the most accurate closed loop control.

- Schemes with rate feedback and a digital integrator (Scheme 4, 11, 18) would provide slightly less accurate closed loop control. Rate feedback schemes with an analog integrator (Schemes 5 and 7) would be even less accurate.

- Torque motor schemes without an integrator upstream of the torque motor (Schemes 6, 8, and 9) would provide very inaccurate closed loop control due to torque motor null shifts.

- Stepper motor schemes without feedback around the stepper motor (Schemes 12 and 13) would provide very inaccurate closed loop control due to the resolution of the stepper motor.

- Stepper motor schemes with feedback around the stepper motor and a hydromechanical integrator (Schemes 14 and 15) would have a smaller steady-state error than schemes without feedback. The steady-state accuracy is directly related to the feedback accuracy.

- Solenoid schemes with digital feedback and a hydromechanical integrator (Schemes 19 and 20) would provide less accurate closed loop control than the solenoid schemes with digital feedback and a digital integrator (Schemes 16 and 18).

- Solenoid schemes without digital feedback (Scheme 21) provide very inaccurate closed loop control.

3. Steady-State Accuracy: Open Loop Control

Steady-state accuracy for open loop control is defined as the accuracy of scheduling fuel flow as required for acceleration and deceleration limiting. This data was calculated only for DOI schemes (1, 2, 3, 6, 10, 12, 16 and 19) which can provide acceleration/deceleration limiting in a full authority electronic control. The fuel flow error is the difference between the requested and actual fuel flow; fuel flow measurement error was included since the measurement is a part of the DOI. The fuel flow errors due to all DOI components were root-sum-squared to determine fuel flow scheduling accuracy for each of the above schemes. The errors were calculated at low requested fuel flows to give an indication of start schedule and off-idle accel schedule accuracy and at high requested fuel flows to give an indication of overtemperature and surge protection at high power.

Schemes without position feedback cannot provide open loop scheduling in a full authority electronic control. Feedback to the digital electronics (Schemes 1, 6, 10, 12, 16 and 19) provides the most accurate open loop scheduling. Analog feedback (Scheme 2) is a close second; hydromechanical feedback (Scheme 3) least accurate.

Based on the component data listed in Table 1, DOI schemes with optical position feedback provide the most accurate open loop control. Schemes with resolver feedback rank a close second; schemes with LVDT feedback rank third.

4. Steady-State Stability

Steady-state stability is indicated by the steady-state limit cycle of the controlled gas turbine engine parameter, low rotor speed. Limit cycles result from digital-to-analog and analog-to-digital converter resolution, component hysteresis, and fuel valve noise due to mechanical

vibration of the fuel control. The limit cycles were determined by observing speed stability several seconds after a small power lever step was run with the simulation. The range of limit cycle variation was determined by root-sum-squaring the change in limit cycle amplitude due to component variation for each DOI component.

None of the DOI schemes showed any undesirable limit cycling that was inherent to the particular components of the scheme. Components and gains of all the schemes were sized for adequate control loop stability.

Initial results of the stability analysis indicated that the stepper motor schemes would exhibit some undesirable limit cycling. This analysis resulted from the ground rule that all schemes be capable of providing stop-to-stop fuel valve motion in one-half a second. This ground rule posed no problem for the torque motor or solenoid schemes, but did complicate the analysis of the stepper motor schemes. The current stepper motor state-of-the-art for a gas turbine fuel flow control application is 500 steps/second; a half second stop-to-stop would use only one-half the total range, or 250 steps. Because early simulation analysis showed undesirable limit cycling from this coarse resolution, the analysis of the stepper motor schemes was based on a 500 step resolution. This corresponds to either a one second stop-to-stop, or advancement in the stepper motor state of the art to 1000 steps/second.

5. Results of Performance Evaluation

The performance evaluation (Table 4) identified the top five DOI schemes (Schemes 1, 2, 10, 16, and 19) based on transient response, closed loop and open loop accuracy, and steady-state stability. These schemes all had two or three sub-schemes; only the best one was included in the final evaluation. The five top schemes are capable of providing both closed loop governing and open loop accel/decel fuel flow limiting in a full authority electronic control. Other DOI schemes in the trade study were satisfactory for either closed loop or open loop scheduling but not both.

H. FAILURE MODE AND EFFECTS ANALYSIS

Two DOI schemes were selected for a failure mode and effects analysis (FMEA) by the control manufacturers. The two schemes were chosen based on the results of the reliability analysis, the life cycle cost study, and the performance evaluation.

Hamilton Standard performed an FMEA on Scheme 16 with optical feedback. The FMEA was conducted on just the components of the digital output interface plus the software required for the adaptive logic in the electronic controller. The results indicated a DOI component failure rate (excluding software failures) of 11.0 failures per million hours, with a system failure rate of 7.5 failures per million hours due to the redundancy provided by the dual wound solenoids and the adaptive nature of the drive logic.

Bendix performed an FMEA on Scheme 1 with resolver feedback. The FMEA was conducted on the digital output interface components plus many other elements of a digital electronic control system including the power supply. The results indicated a DOI component failure rate of 22.3 failures per million hours. The system failure rate would be 12.2 failures per

million hours because the software can switch to a backup control mode if the resolver or the resolver-to-digital converter in the feedback failed. In the backup control mode, the integrator in the software would be bypassed and operation would continue with the interface configured as Scheme 9 with a torque motor driving a hydromechanical integrator.

Both FMEA's were reviewed by the Pratt & Whitney Aircraft Reliability and Maintainability groups. The reliability group commented that a triple redundant majority vote solenoid system might be considered for better operational reliability in the Hamilton Standard scheme. The reliability specialist pointed out that there could be a failure mode in the demultiplexer/torque motor of the Bendix scheme that calls for maximum flow. This could cause an overtemperature or a stall if the electronic control does not switch to a safe mode or shut down.

The maintainability group reviewed both FMEA's and suggested the following for consideration in future designs:

1) From a maintenance viewpoint, it would be advantageous to have the electromechanical device (torque motor, stepper motor, or solenoid) mounted separately from the hydromechanical unit for easy changeout.

2) The fiber optic position sensor in the HSD scheme should be easily removable from the hydromechanical unit.

3) Any failure should be annunciated even if the system performance is not affected. This allows maintenance to be scheduled at a convenient time.

The first two suggestions would have to be evaluated in the context to the total system maintenance requirements but the annunciation of failures should be part of any electronic control system.

I. FINAL EVALUATION

The top five DOI schemes from the performance evaluation were compared in a final evaluation based on reliability, performance, life cycle cost, and sampling requirements. The five schemes were ranked from 1 to 4 in each of the above four categories, and the ranking was multiplied by the weighting factor. Weighting factors used were three (3) for reliability and performance, two (2) for life cycle cost, and one (1) for sampling requirements. This combination of weighting factors places the highest weighting on reliability because reliability is both an independent category and a factor in the life cycle cost.

Sampling requirements of the DOI schemes were determined from the computer simulations. Sampling time was increased from the baseline of 15 milliseconds until small step response became either sloppy or unstable. Open loop sampling requirements were established by increasing the sampling time until Wf/Pb ratios overshot the accel schedule during a snap accel from idle. Sampling time limitations for both closed loop and open loop control are tabulated in Table 5.

The performance of the top five DOI schemes was evaluated at two operating conditions – high power at sea level static, and cruise power at 9144 meters (30,000 feet), .8 Mach number – to establish performance rankings for the final evaluation. The performance evaluation of the top five schemes used the same procedure as the performance evaluation which compared all twenty-one DOI schemes. The performance of all five schemes was found to be very similar at the sea level static condition (Table 6), with Schemes 2, 10, 16 performing slightly better than Schemes 1 and 19. The performance evaluation at altitude cruise (Table 7) showed a trend similar to sea level static results, but the differences between the top three and bottom two DOI schemes were more pronounced. Sea level and altitude performance were weighted equally in the final performance evaluation. The final tabulation was made by adding the totals for the sea level and altitude conditions and then establishing a combined ranking for each of the DOI schemes (Table 8).

Sampling requirements were evaluated by weighting closed loop and open loop requirements equally. As shown in Table 9, DOI Scheme 2, which uses analog (continuous) feedback can run at a longer sampling interval than the other four schemes. Open loop limiting requires faster sampling than closed loop control. Accel/decel limiting requires faster sampling than most open loop applications because no accel/decel schedule overshoot can be accepted. A nozzle or vane scheduling control could run at a longer sampling interval if schedule overshoot is permitted.

Reliability and life cycle cost were ranked by assigning a four (4) to the worst of the five schemes, and one (1) to the best; and the rest were interpolated linearly in between those extremes. The reliability and life cycle cost rankings are tabulated as part of the overall evaluation presented in Table 10.

The final rankings, which are tabulated in Table 10, identified DOI Scheme 16 as clearly the best overall configuration.

J. TRADE STUDY CONCLUSIONS AND RECOMMENDATIONS

The most promising DOI scheme (16) is a digital effector, which uses on-off solenoids driven directly through a driver circuit by a digital word command. The software includes an integrator and adaptive logic. Optical position feedback to the digital electronics was selected for fuel valve position measurement.

Solenoids have been widely used in gas turbine controls, but only for non-modulated control components like bleed valves, shut-off valves, etc. The use of solenoids to control a fuel valve or a vane or nozzle position actuator is a new control concept. Solenoids have only two steady-state positions corresponding to the energized and de-energized electrical states. The on-time is modulated to regulate the servo flow to the actuator. On-time is controlled by timing logic in the digital controller which commands the on/off drive signals.

Based on the results of the trade study, it was recommended that the scheme 16 digital effector with optical feedback be selected for the preliminary and final design tasks in the program. Hamilton Standard was selected to perform these designs because they had conceived the digital effector scheme and had been involved with the development of an optical position sensor. NASA concurred with this recommendation.

IV. DESIGN OF THE SELECTED DOI SCHEME

The trade study was followed by the preliminary and final designs of a prototype digital effector with optical feedback which is intended to operate the fuel metering valve of a gas turbine full authority electronic controller. The specific elements of this system include: (1) a digital effector to interface with the fuel metering valve in a hydromechanical fuel flow package, (2) an optical position feedback device, (3) the electrical interface circuits between the controller/effector and the optical sensor/controller, and (4) the adaptive logic portion of the controller software required to operate the digital effector.

Hamilton Standard designed the hardware for the digital effector interface. Pratt & Whitney Aircraft developed the software and performed dynamic analysis of Hamilton Standard's preliminary and final designs.

A. DIGITAL EFFECTOR DESIGN

The digital effector will position the fuel metering valve by discrete velocity commands from the digital controller. When activated, the solenoid valves in the digital effector will port the supply pressure on one side of the fuel metering valve to drain pressure, causing a pressure differential on the servo actuating piston to translate the fuel valve in the corresponding direction. Closing the solenoid valve restores supply pressure to the servo piston and stops fuel valve translation.

1. Solenoid Valve Selection

Solenoid valves for the digital effector were selected based on response, pressure limitations, and flow capacity. The solenoids are available as standard items from the manufacturer and are capable of operating at pressures up to 862 newtons/cm^2 (1250 pounds per square inch). The solenoids selected are among the fastest responding in this pressure range, with a response time of .003 to .005 seconds from off to full flow. The solenoid valves were sized to slew the fuel metering valve at the maximum required velocity of 2.286 cm/second (.9 inches/second).

2. Solenoid Configuration

The solenoid configuration for the digital effector was selected based on performance and reliability considerations. Two-solenoid and three-solenoid configurations were initially considered. The two-solenoid configuration would have fewer components and therefore a higher parts count reliability than the three-solenoid configuration. The three-solenoid configuration would provide built-in redundancy for a single solenoid failure.

The two-solenoid configuration is a three-position system because three choices of fuel metering valve velocity are possible: increase fuel flow at maximum rate, decrease fuel flow at maximum rate, and zero velocity. A schematic of the two-solenoid configuration is shown in Figure 6. When the increase solenoid is energized, the solenoid valve will port servo supply pressure (PS) to drain pressure (PD). This would drop the pressure on the right side of the fuel metering valve, causing the valve to translate to the right. Energizing the decrease solenoid would cause translation to the left. When both solenoids are de-energized, supply pressure (PS) would be applied to both sides of the fuel metering valve to null its velocity.

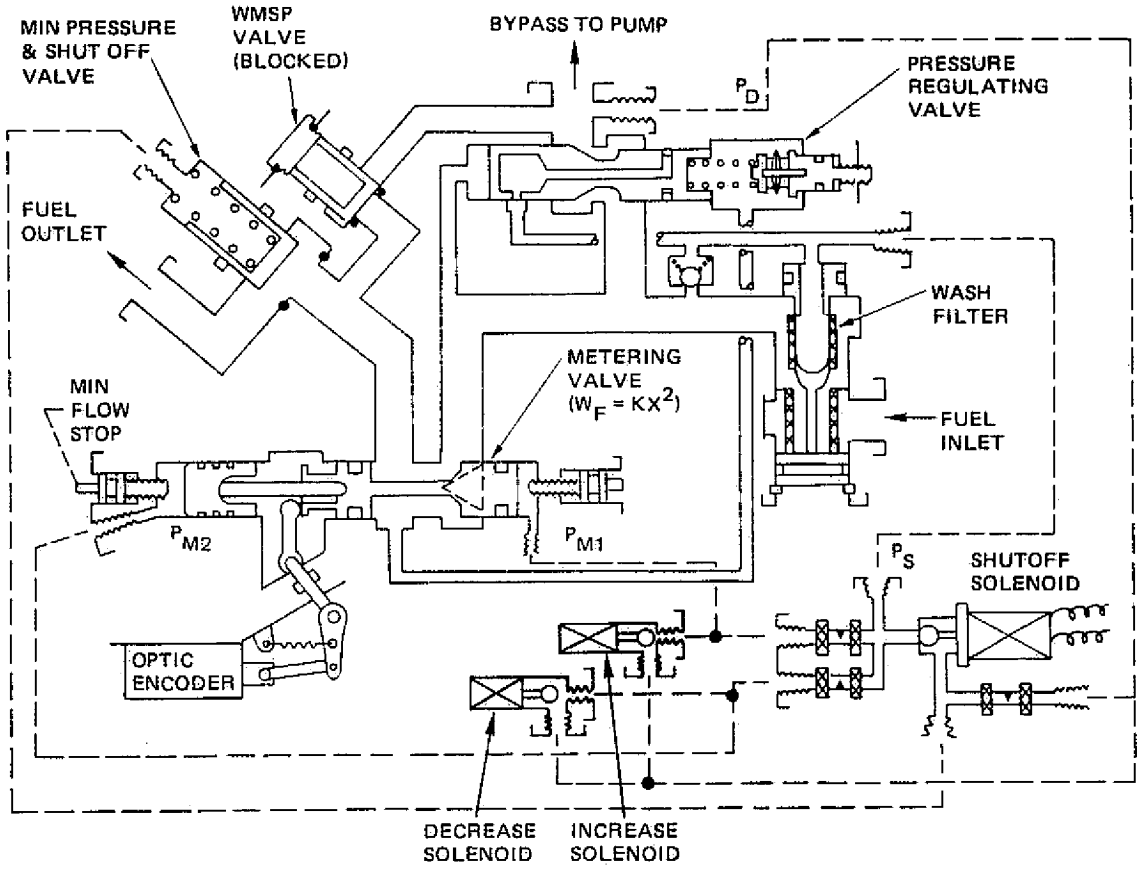

Figure 6 Two-Solenoid Configuration

The three-solenoid configuration is a triple redundant majority vote system. Any single solenoid failure will be automatically overridden because the position of any two of the solenoid valves determines the control action independent of the position of the third solenoid.

Figure 7 shows a schematic of the three-solenoid configuration. The left side of the fuel metering valve has a half area servo and a regulated hydraulic supply pressure. The pressure on the right side of the fuel metering valve is controlled by the solenoids. When two or three solenoid valves are closed, the controlled pressure is greater than one-half of the regulated supply pressure . The fuel valve would translate to the left because the larger area servo on the right side of the metering valve provides a net force to the left. When two or three solenoid valves are opened, the controlled pressure drops below one-half of the regulated pressure causing the metering valve to translate to the left.

The three-solenoid configuration has a major drawback: it is a two-position system with only two choices of fuel metering valve velocity – increase or decrease fuel flow at the maximum rate. There is no zero velocity state. For steady-state operation, the solenoids must be energized for one-half of every digital electronic control cycle and then de-ener-

gized to maintain an average net zero velocity. The lack of a zero-velocity state causes fuel flow limit cycling and continuous solenoid cycling. This can be expected to greatly reduce operational life of the solenoids and the reliability of the digital effector.

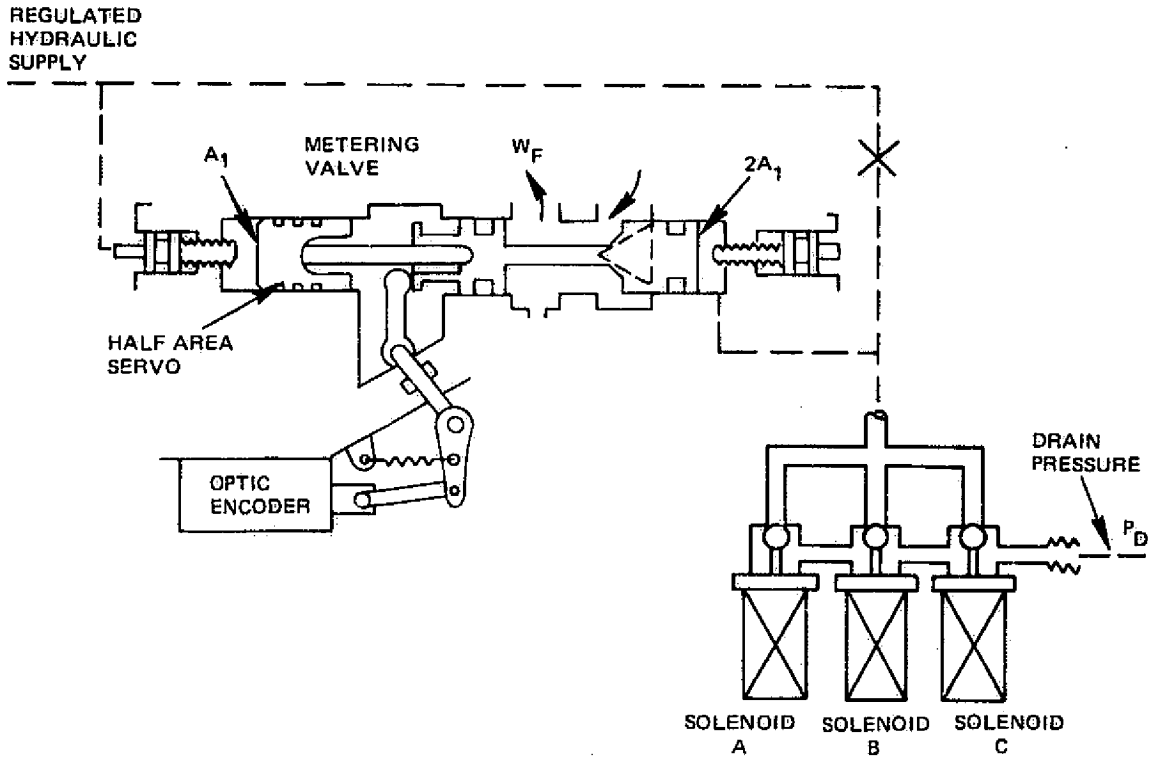

Figure 7 Three-Solenoid Configuration

The two-solenoid configuration was selected for its reliability and performance advantages over the three-solenoid configuration.

Dynamic analysis of the two-solenoid scheme indicated that a solenoid failing open would cause an abrupt fuel flow change and a loss of capability to increase (or decrease) fuel flow. A solenoid failing closed would also cause a loss of capability to move the fuel metering valve in one direction. A solenoid failure with the two-solenoid configuration could result in either an engine unable to accelerate above idle power, or an over-fueled engine which would have to be shut down through the shut-off solenoid.

At the Task 2 Preliminary Design Review, Pratt & Whitney Aircraft recommended a four-solenoid configuration consisting of two parallel solenoids on each side of the fuel metering valve to provide improved engine protection during development testing of the digital effector. A production version of the digital effector would require development of more reliable solenoids thus allowing use of a two-solenoid configuration. NASA agreed with this recommendation and the final design was performed using the four-solenoid digital effector concept.

A schematic diagram of the four-solenoid configuration is shown in Figure 8. For normal operation, the solenoids on each side of the fuel metering valve will be operated in pairs. With all four solenoids de-energized, the metering valve does not translate. Energizing the decrease solenoids would cause the metering valve to translate to the left; energizing the increase solenoids would cause the metering valve to translate to the right. No single solenoid failure would cause a steady state fuel flow change or a loss of capability to increase or decrease fuel flow.

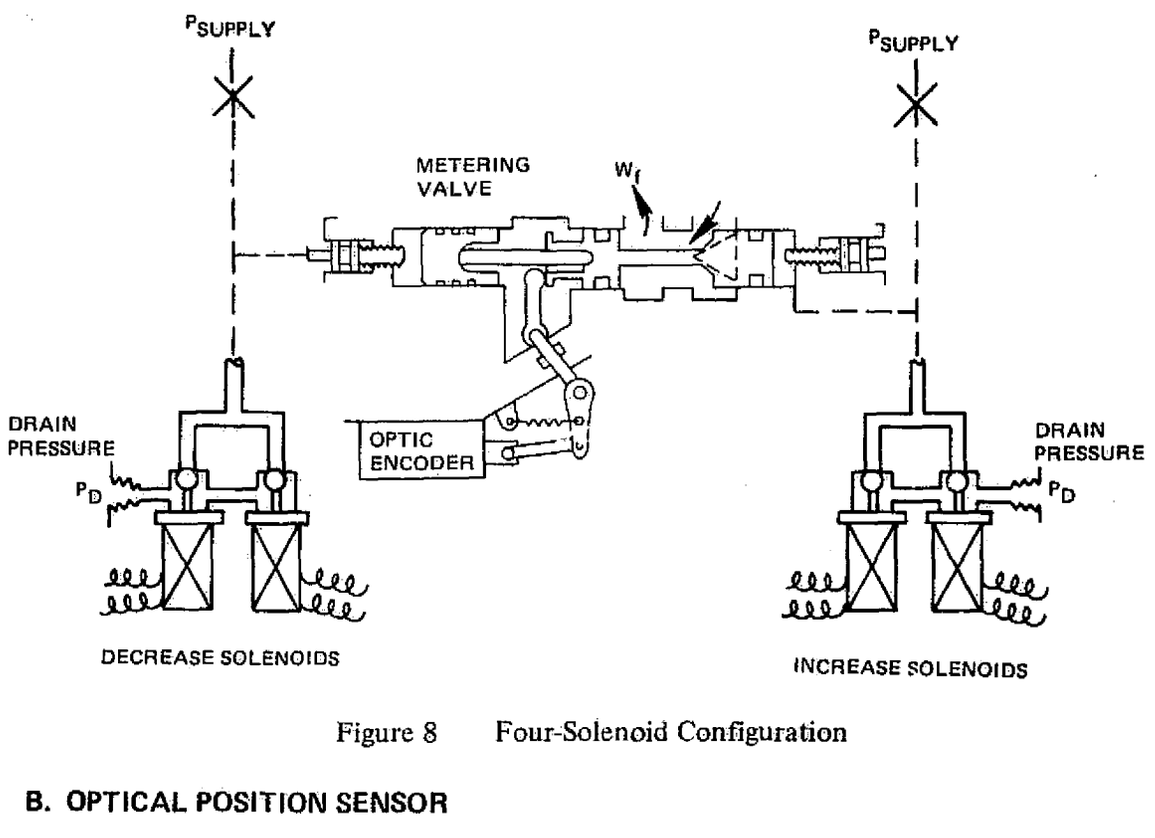

Figure 8 Four-Solenoid Configuration

B. OPTICAL POSITION SENSOR

An optical position sensor was designed to meet the accuracy requirements of a fuel metering valve position measurement device. The design was based on state-of-the-art technology as applied to a gas turbine fuel flow control and was chosen to demonstrate optical position measurement of a gas turbine fuel valve.

The optical position sensor includes a mask that encodes the position into an 8-bit signal. The encoder mask is mechanically linked to the fuel metering valve and slides between the optic heads. The optic source and receiving heads consist of individual fiber bundles for each channel to minimize optical power losses in the head assembly. The source head contains eight fiber optic bundles which are illuminated by a light-emitting diode triggered by a signal from the electronic control. The opposite head has eight optical receiver lines which are precisely aligned with the source heads. Interruption of the light path between the heads by the etching on the plate provides the digital indication of position.

The hole size for the least significant bit of the encoder mask is .254 x 1.016 mm (.010 x .040 inches). An eight-bit Gray code format selected for the encoder mask enables a mask position resolution of .127 mm (.005 inches) by overlapping adjacent bits on the mask. The difference between Gray code and binary codes is tabulated in Table 11.

The mask resolution in combination with the source and receiver head size of .127 x 1.016 mm (.005 x .040 inches) results in a .127 mm (.005 inch) resolution of the position measurement. A .127 mm (.005 inch) fuel valve position measurement resolution is equivalent to 113 kilograms per hour (250 pounds per hour) at high power and 38.5 kilograms per hour (85 pounds per hour) at idle (due to the non-linear metering valve characteristic) and would not be accurate enough for a feedback signal. A 2.5:1 linkage ratio between the optical sensor and the fuel metering valve was designed to provide a .051 mm (.002 inch) resolution of the fuel metering valve position measurement.

Three preliminary design concepts for the optical position sensor utilized a linear encoding mask. The mask would slide on a row of bearings driven by a piston linked through a rotational lever which is in turn linked to the fuel metering valve. A tension spring in the mask would keep the system loaded, eliminating hysteresis. However, the spring acting on the unsupported mask would tend to distort the mask.

A fourth preliminary design utilized the encoder mask as a sector of a disk which is mounted directly on the rotational lever. This design eliminates the piston and the bearings. The spring in the sector mask system acts on the lever and has a lower spring constant than the spring required to load the piston in the linear mask system. The lower spring constant provides less loading on the fuel metering valve. The sector mask design, which is shown in Figure 9, was selected for the final design.

C. HYDROMECHANICAL FUEL FLOW TEST PACKAGE

The fuel flow package for the digital effector system is a hydromechanical control unit that consists of fully developed gas turbine engine fuel metering elements (fuel metering valve, pressure-regulating valve, wash filter, minimum pressurizing shutoff valve, and shutoff solenoid) modified to incorporate four solenoid valves and the metering valve position follower link to the optical position sensor and the resolver. Figure 10 shows the schematic of the flow package and Figure 11 shows the physical arrangement.

1. Fuel Metering Valve

The fuel metering valve is a translating, nonlinear window-type valve that is positioned by discrete velocity commands from the solenoid valves. The sequencing of high-speed control solenoids regulates servo flow, which controls metering valve velocity to the equal area servo pistons on each side of the metering valve. Three choices of velocity are available: zero, increase fuel flow at maximum velocity, and decrease fuel flow at maximum velocity.

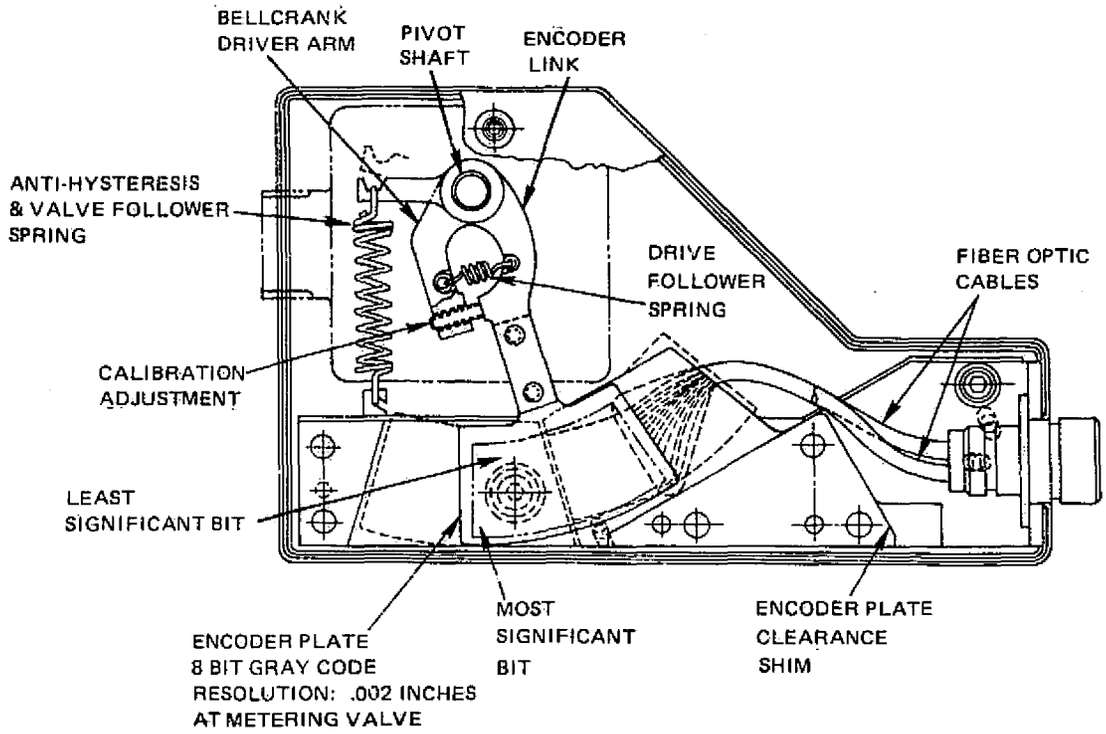

Figure 9 Schematic of Optical Position Sensor

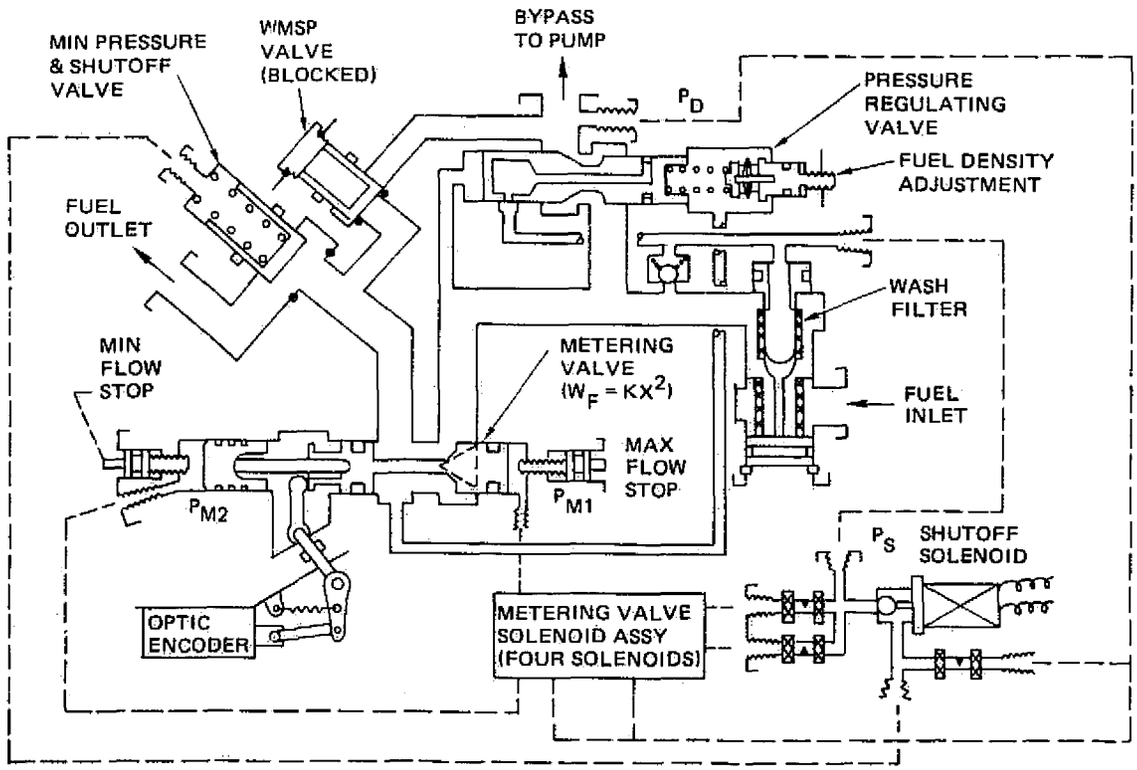

Figure 10 Schematic of Fuel Flow Package

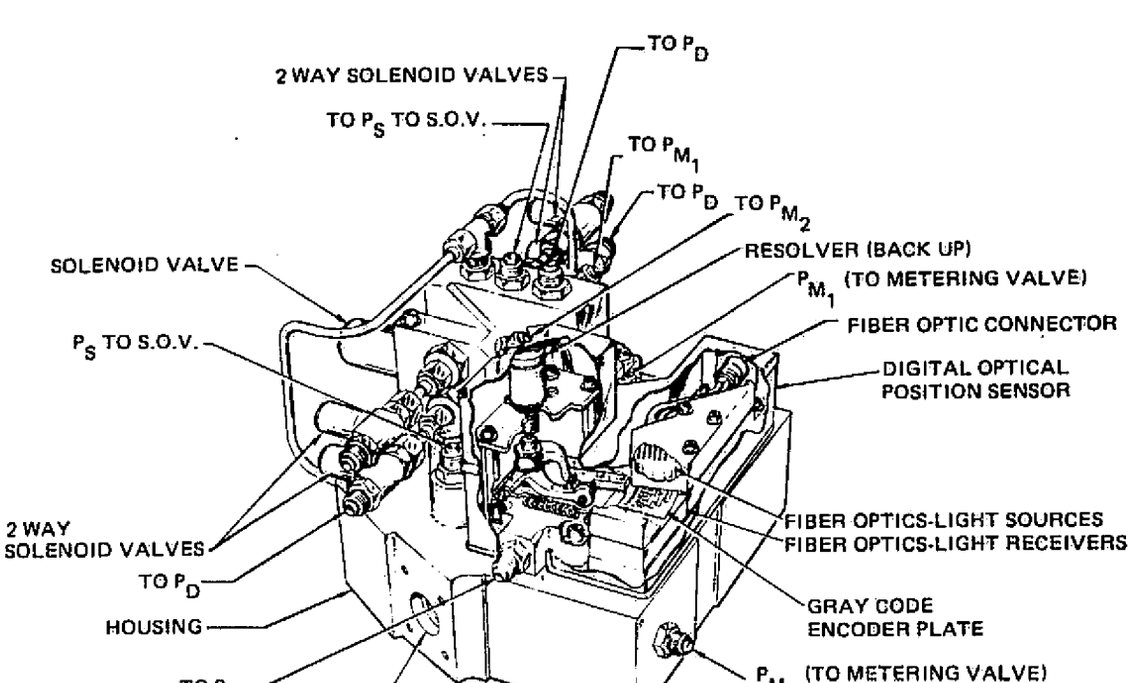

Figure 11 Fuel Flow Package Including the Solenoid Actuators and the Optical Position Sensor

2. *Minimum Pressurizing Valve*

The minimum pressurizing valve at the control outlet prevents fuel from flowing until a minimum pressure level of 206.8 newtons/cm^2 (300 pounds per square inch) referenced to control-body pressure has been achieved within the control. This assures that the pressure regulating valve will have adequate operational pressure for accurate pressure regulation. The valve consists of a spring-loaded piston seated against a trapped O-seal to achieve leakage-proof sealing. Control-body pressure is sensed on the spring side of the piston. During startup, with the shutoff solenoid energized, the valve will not open until the pressure on the valve face exceeds control-body pressure by the equivalent spring load pressure. When the solenoid is de-energized, supply pressure is ported to the spring side of the piston to close the valve and shut off fuel.

3. *Filter and Relief Valve*

A 20-mesh, .381 mm (0.015-inch) diameter wire, coarse screen barrier filter is located at the fuel inlet. A wash-type 40-micron (.00158 inch) fine filter downstream of the coarse filter gives better than 40-micron (.00158 inch) filtration for servo supply pressure. The wash velocity keeps the filter surface clean and also tends to keep the contamination particles from making the turn to pass through the filter. In combination with the very smooth Regimesh screen, this feature provides filtration which closely approaches 20-micron (.00079 inch)

filtering capability. As the screen is continuously washed, no maintenance is necessary. A simple spring-loaded ball relief valve will bypass the fine filter if the pressure drop across the filter exceeds a 10.34 newtons/cm^2 (15-pounds per square inch) pressure level. Barrier filters are also provided for all small control orifices for protection during filter bypass operation.

4. Position Sensor

The position sensor consists of two completely independent systems — an optical position sensor and a resolver. The resolver was included at NASA's request and will be used for instrumentation purposes and possibly as a backup in the software of the electronic controller for the optical position sensor. Each is driven directly by the fuel valve follower shaft and is independently calibrated relative to the fuel metering valve position. The fuel valve follower converts the linear position of the valve to a rotary position in the follower shaft which can be used directly by both feedback devices.

The resolver is attached directly and in-line with the follower shaft and rotates with the shaft. Calibration of the resolver is accomplished by rotating the resolver housing with clamps loosened.

D. INTERFACING ELECTRONICS

The electronic and optical interface circuits are designed to be packaged in a single interface unit (IFU) with provisions for nitrogen or air cooling during engine test-cell operation to meet the specified 366°K (200°F) ambient environment.

The interface unit includes the solenoid drive circuits, the optic-electronic interface, a resolver-to-digital converter, and a serial data transmitter.

1. Solenoid Drive Circuits

Four separate solenoid drive circuits have been designed. A four-bit word controlling these drives is output from the digital processor, into a four-bit parallel register. Each of the parallel outputs of the register controls one solenoid drive. When a register output is high, the corresponding solenoid is turned on and will remain energized until the register is updated by the computer with a new word containing a low bit in that position.

Each parallel output of the register controls a switched current source. The current source will provide a relatively constant drive to the output stage. Therefore, the drive circuit power requirements for the system power supply will also remain relatively constant.

2. Optic-Electronic Interface

The optical position sensor consists of a light-emitting diode (LED), LED drive circuit, a fiber optic system and encoder plate, and an eight-channel light-sensitive receiver circuit. Infrared radiation from the LED is transmitted through the fiber optic system to the encoder plate, which is mechanically attached to the shaft of the metering valve. The infrared radiation is allowed to pass through the encoder plate to one or more of the fiber optic channels

on the receiver side of the encoder plate as a function of the metering-valve shaft position. The presence or absence of radiation in the receiver fiber optic bundles is sensed by eight parallel photodiodes and this data is latched into a logic register where it is then available for use by the system controller.

In order to make an accurate determination of the position of the encoder plate which represents the transition between "on" and "off" for any channel, it is necessary to maintain a constant optical output power level from the LED. The conversion efficiency of the LED (optical output power versus input current) is a function of LED temperature and it is therefore necessary to control the current into the LED as a function of LED temperature. This is accomplished by mounting a thermister in thermal contact with the LED and using the temperature variation of the thermistor resistance to control LED drive current.

In order to obtain enough infrared radiation from the LED to assure reliable detection through the optical system losses, it is necessary to drive a substantial current through the LED. Continuous operation of the LED at the required current levels would result in large system power demand and excessive heat in the LED. It is, therefore, desirable to power the LED with fairly narrow current pulses at a low-duty cycle (powered only one percent of the time). A triggering signal from the digital processor will activate the LED.

A simplified schematic of the circuit proposed to drive the LED is shown in Figure 12. This circuit uses a thermistor to provide a temperature-dependent drive current to the LED and allows the drive current to be pulsed.

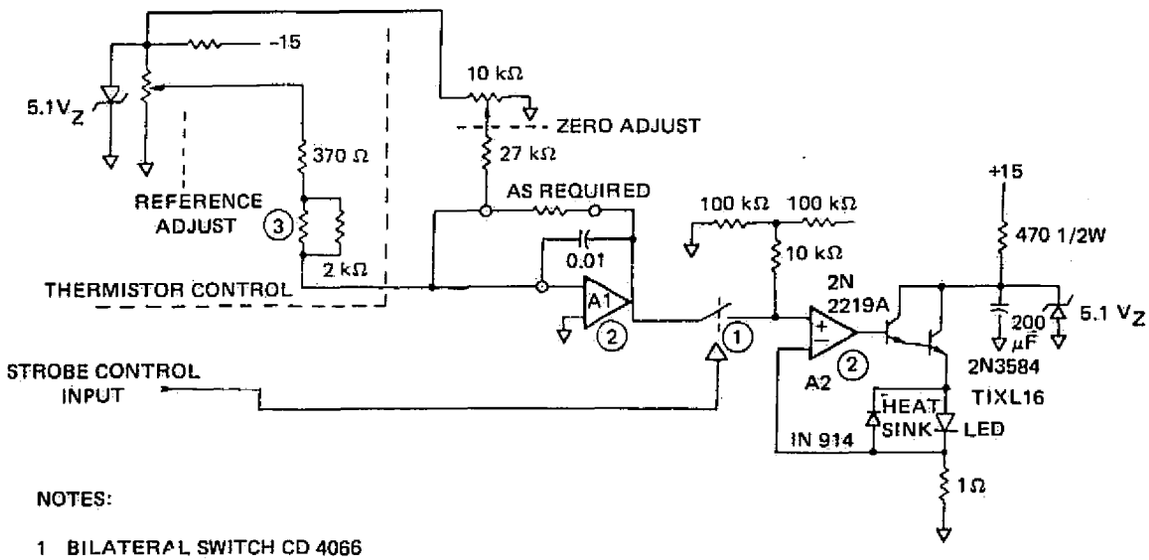

NOTES:

1 BILATERAL SWITCH CD 4066

2 A1 AND A2 1/4 OF LM124

3 THERMISTOR TYPE VECO 202 D208JC
2 kΩ AT 25°C

Figure 12 Simplified Schematic of Light-Emitting Diode (LED) Drive Circuit

A simplified schematic of the circuit proposed for use as the optical receiver is shown in Figure 13. In this figure only one of eight identical receiver channels is shown. The SGD 040 A photo diode is the detector element. Since the inverting input of op-amp A1 is a virtual ground, the detector diode (A) has a constant +15V reverse bias applied. This reverse bias causes an increase in detector sensitivity and increases the speed of response of the diode. Also shown is the guard-ring diode (G) which is fabricated on the same substrate as the detector diode. The guard ring diode serves to reduce the magnitude of the detector diode dark current.

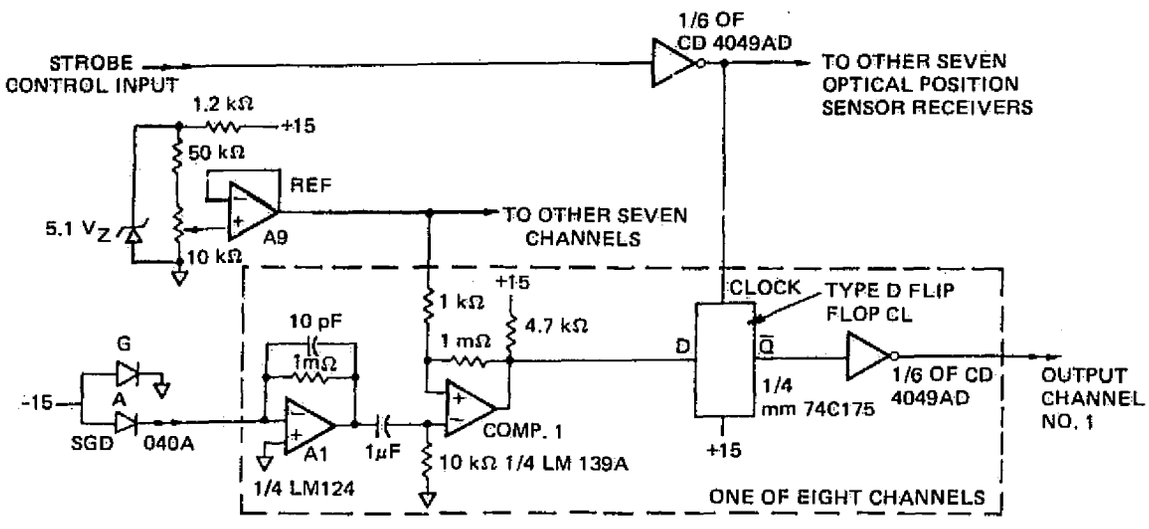

Figure 13 Optical Position Sensor Receiver Circuit

Op-amp A1 functions as a current-to-voltage converter with a gain of 1 mV/na. The current through the detector diode (leakage current plus radiation induced current) is, therefore, converted to a voltage at the op-amp output.

The output voltage of A1 is AC coupled to the input of the voltage comparator. The output of A1 caused by the detector leakage current is essentially DC and is blocked by the 1-uf coupling capacitor: The signal due to the pulsed LED output is passed to the comparator input.

The threshold voltage of the comparator is set by the output voltage of A9 and is adjustable to allow compensation for variations in LEDs and fiber optic assemblies. Included in the comparator is a small amount of hysteresis to assure stable operation when the input signal is near threshold.

The output level of the comparator is latched into the output flip-flop at the completion of the LED stroke pulse and the flip-flop then presents a stable signal to the system controller.

3. *Resolver-to-Digital Converter*

This circuitry provides the resolver excitation and a 12-bit resolver-to-digital converter. The resultant conversion accuracy is better than ±10 minutes.

4. *Serial Data Transmission*

The position data from the Optical Position Sensor is available as eight parallel bits and the corresponding data from the Resolver-to-Digital Converter is presented as 12 parallel bits. In order to avoid the necessity for 20 line pairs to carry this data from the sensor electronics to the control computer, the data is converted to a serial format at the IFU, transmitted over two line pairs, and reconverted to parallel format for use by the digital processor.

The data at the IFU is first strobed in parallel into a shift register. The contents of the shift register are then clocked out onto the data transmission line. A line pair carrying the shifting clock is also brought out of the IFU electronics.

The data line pair and clock line pair are brought into a shift register at the interface to the digital processor. The data is shifted serially into a register by the clock line. At the completion of the shift clock burst, the data is strobed into a parallel register where it is available to the digital processor.

5. *Interconnecting Cabling*

The interconnecting cabling between the digital effector assembly and the IFU consists of a six-foot optical cable which will connect the optical interface circuitry to the optical encoder connector. Also provided is the electrical cabling connecting the four solenoids to the IFU, and the electrical cabling connecting the resolver to the IFU. Cabling is also provided between the IFU and the digital processor for bench testing.

E. SOFTWARE LOGIC FOR THE ELECTRONIC CONTROLLER

The dynamic simulation of DOI Scheme 16 used in the trade study was modified to include the detailed dynamics of the digital effector and metering valve actuator. This modified simulation was used to design the logic which controlled the operation of the digital effector.

1. *Dynamic Simulation*

A block diagram of the digital effector and actuator dynamic simulation is shown in Figure 14. Solenoid dynamics and friction, and loading from the optical feedback linkage were simulated. The .051 mm (.002 inch) resolution of the optical fuel valve position sensor was also incorporated into the simulation. A computing interval time of .1 milliseconds was required to simulate the high frequency dynamics of the digital effectors, servo flow, and fuel metering valve actuator.

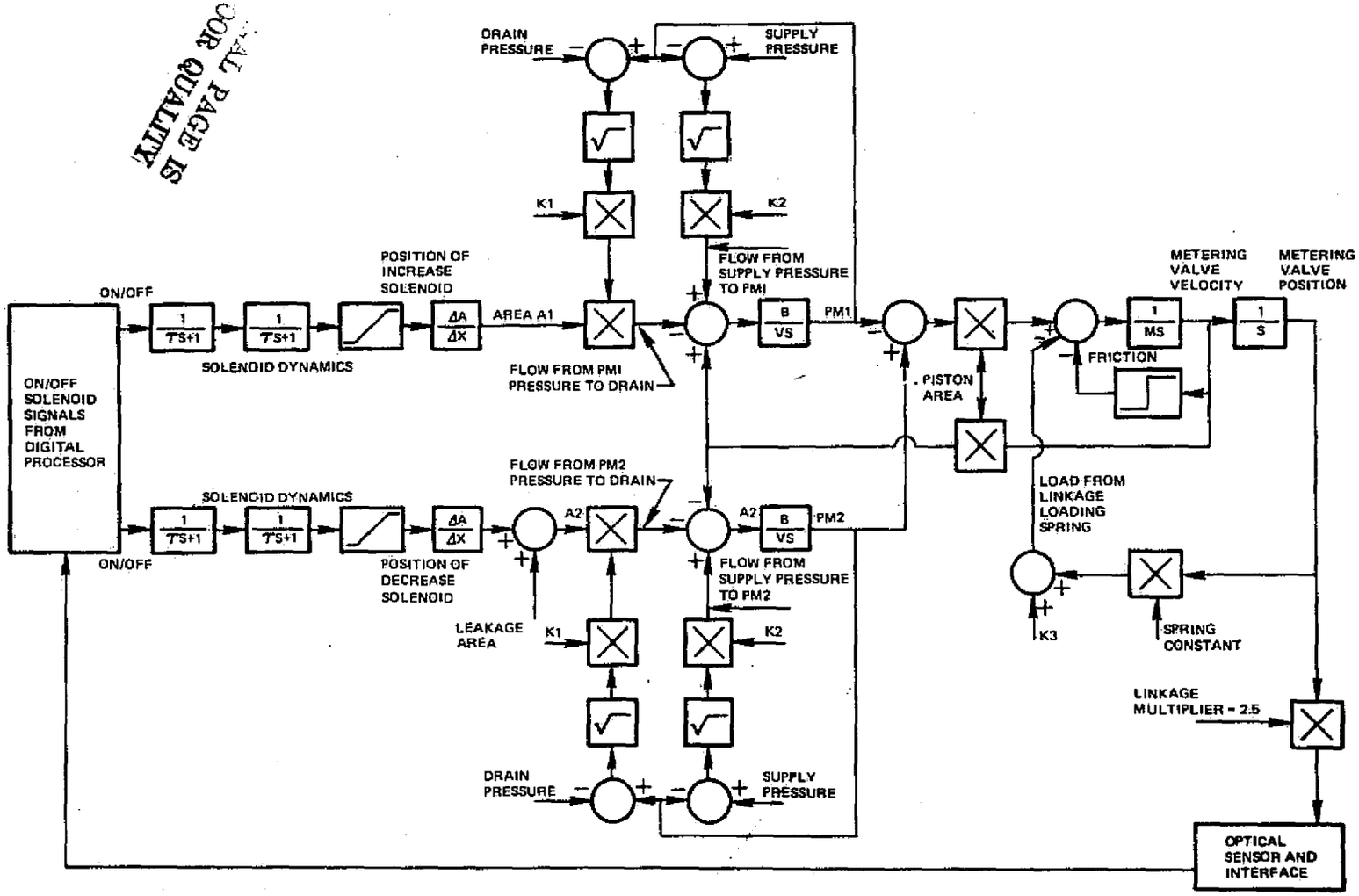

Figure 14 Block Diagram of Digital Effector and Metering Valve Actuator

2. *Adaptive Logic*

A schematic of the electronic controller software is shown in Figure 15. The controller uses adaptive logic to control the dynamic response of the fuel metering valve. The adaptive logic, which is shown in Figure 16, varies a software gain in the metering valve position control loop (Figure 17) to control the open loop gain to a desired value. The variable software gain, which is called the adaptive gain, can be calculated from the constant software gains and the gain of the hardware portion of the control loop. Appendix B shows the calculation of the adaptive gain.

The original design of the adaptive logic used a constant desired loop gain. Simulation data with the two-solenoid configuration and the original adaptive logic is shown in Figure 17. Transient response is good with acceptable steady-state stability, although some fuel flow spiking will occur. The solenoids would cycle 10 times per second in steady-state.

The adaptive logic was revised to incorporate a desired loop gain which varies with the metering valve position error (requested metering valve position minus the measured metering valve position) as indicated in the following equation:

$$\text{Desired Loop Gain} = \text{The Lower of } 45 \text{ and } 45\left[\frac{\text{Position error}}{.003}\right]^2$$

By changing the desired loop gain to a function which decreases as the position error decreases, the solenoids are only energized when the position error reaches a certain minimum level. This change will eliminate energizing the solenoids to correct small fuel flow errors and therefore will improve the solenoid life and system reliability.

The above relationship between the desired loop gain and the position error was derived by a trial-and-error process and would reduce steady-state solenoid cycling to 4 times per second, down from 10 cycles per second with a constant desired loop gain of 45. A small power lever step and steady-state at high power with the two-solenoid scheme and the revised adaptive logic is shown in Figure 18.

The adaptive logic includes limiting logic, which is indicated in Blocks A, B, C and D of Figure 16, to prevent the adaptive gain from increasing excessively or too rapidly, resulting in excessive steady-state solenoid cycling. Block A prevents the adaptive gain from increasing excessively if the metering valve position measurement does not change between successive computer cycles. The limits in Block B and the output limits of Block C prevent the gain from increasing too high and also limit the maximum value of the gain. The time constant and rate limits in Block C and the logic in Block D are dynamic limits which prevent the gain from increasing or decreasing too rapidly.

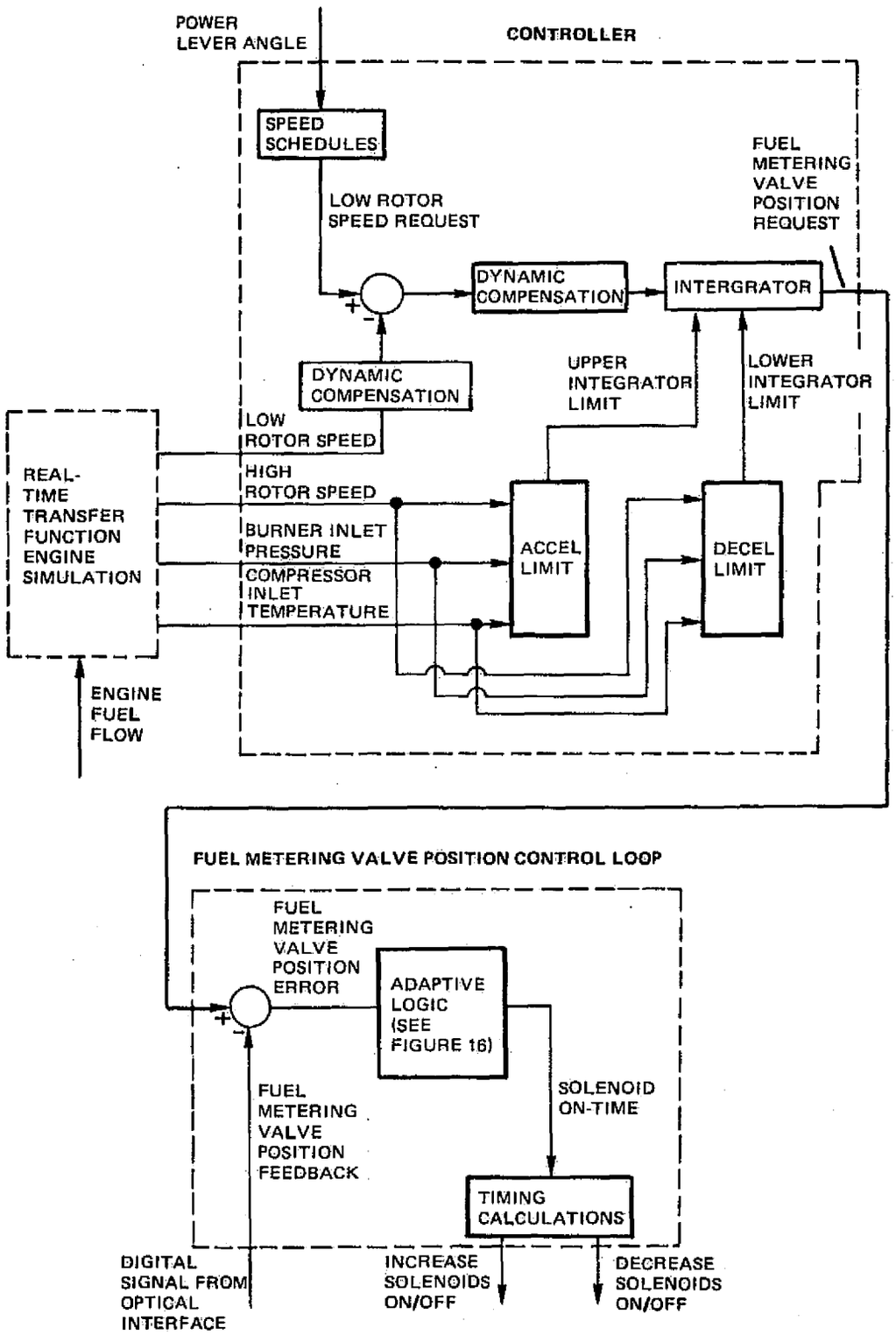

Figure 15 Electronic Control Software Schematic

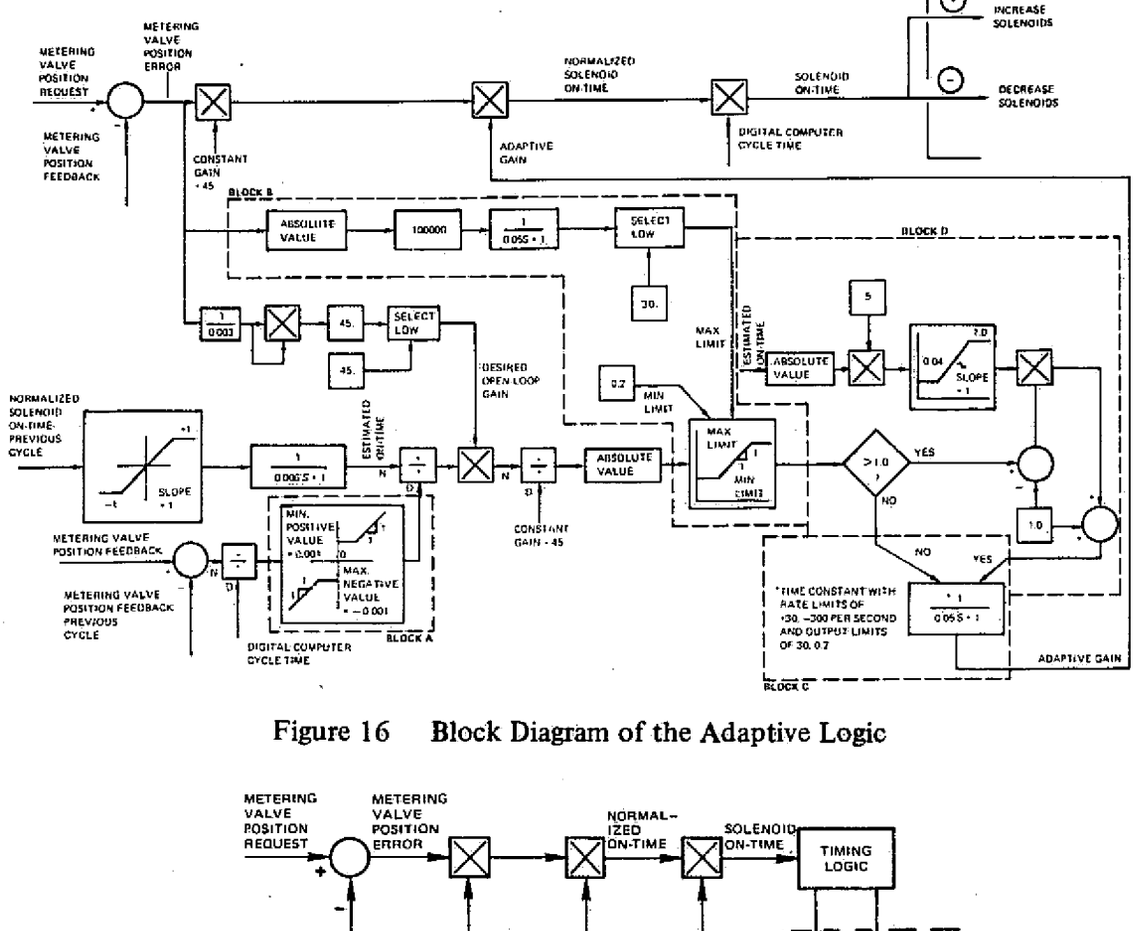

Figure 16 Block Diagram of the Adaptive Logic

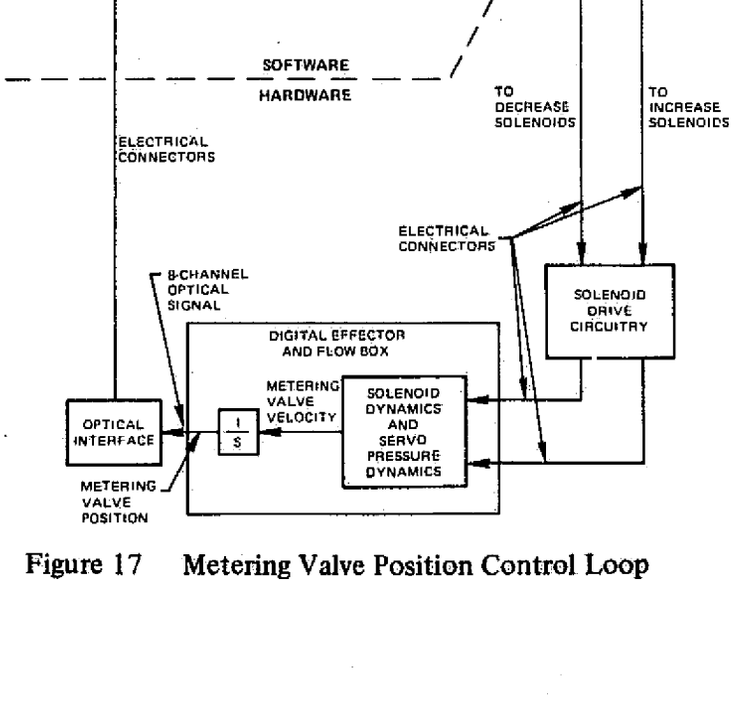

Figure 17 Metering Valve Position Control Loop

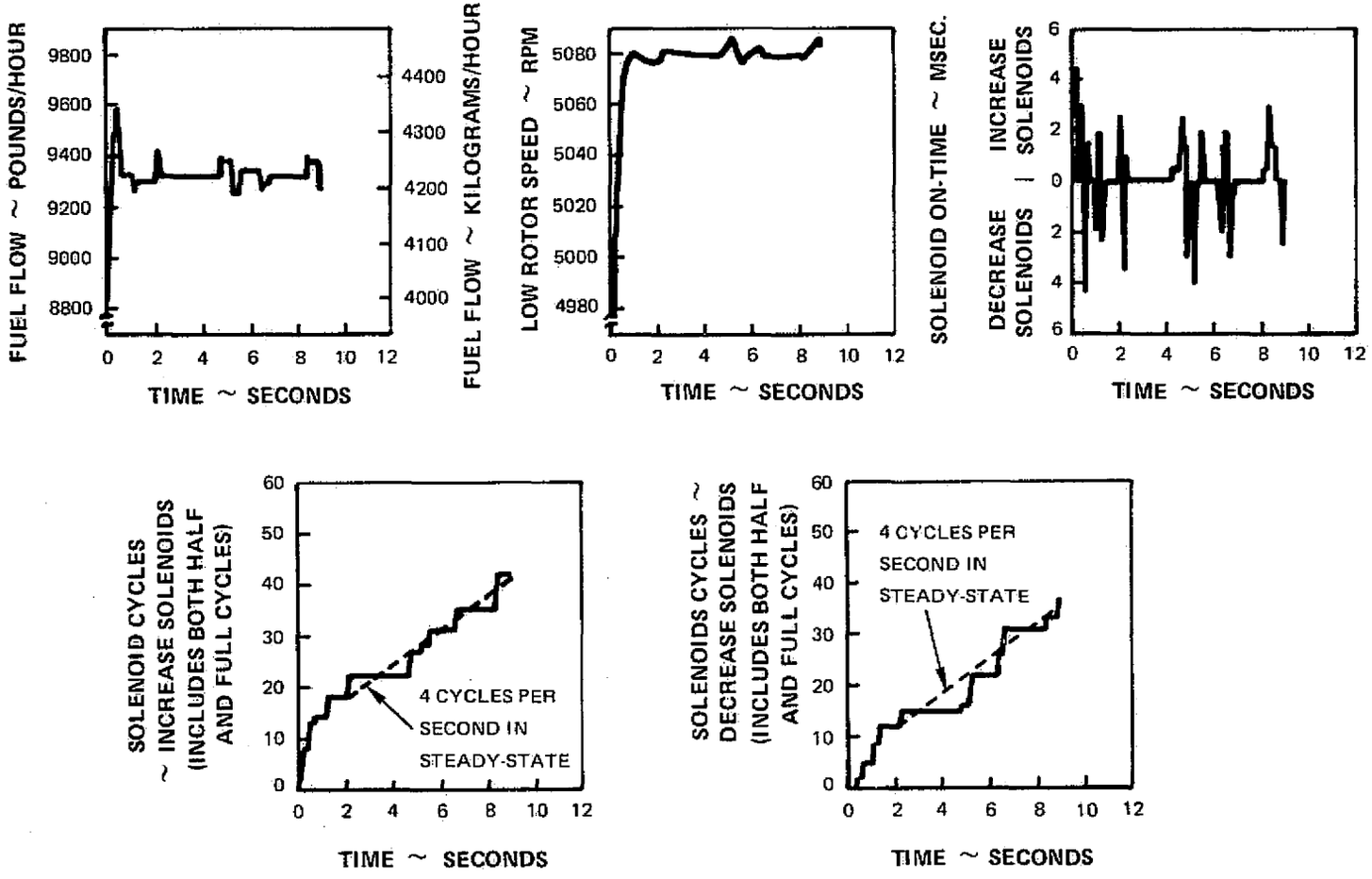

Figure 18 Small Power Lever Step and Steady-State Operation at Sea Level Static, High Power with the Two-Solenoid Configuration and with Revised Adaptive Logic

The adaptive logic will increase the software gain to keep the solenoids energized long enough to overcome the deadband (due to solenoid and metering valve actuator friction) from the metering valve position error to valve velocity. Varying the software gain results in less solenoid cycling than a constant, non-adaptive loop gain by energizing the solenoids less frequently, but keeping them energized for a longer time when they are cycled.

Without adaptive logic, the solenoids in the two-solenoid configuration would cycle 9-10 times per second in steady-state, as shown in Figure 19. Larger steady-state fuel flow and low rotor speed limit cycles result with no adaptive logic. Without adaptive logic, the gain labelled ADAPTIVE GAIN in Figure 17 is equal to a constant 1.0. The constant gain cannot overcome the de-stabilizing effects of the deadband in the forward path and the .051 mm (.002 inch) feedback resolution of the metering valve position control loop.

F. DYNAMIC ANALYSIS OF PROPOSED DESIGNS

Pratt & Whitney Aircraft reviewed Hamilton Standard's preliminary and final designs of the digitial effector and optical feedback. Review of the preliminary designs indicated undesirable failure consequences with the two-solenoid configuration and excessive solenoid cycling at idle. Consequently the final design was changed to incorporate four solenoids and the loading from the optical encoder was reduced to eliminate the excessive solenoid cycling at idle.

1. Dynamic Analysis of Preliminary Design

a. Digital Effector: Two-Solenoid Configuration – Dynamic analysis predicts that the two-solenoid digital effector will provide very fast and stable fuel metering valve response with good engine-control stability. A small power lever transient is shown in Figure 20. Friction from the optical encoder linkage and from the actuator seals will provide adequate system damping. The data shown in Figure 20 was generated with a 12-bit fuel valve position feedback signal to analyze the dynamics of the digital effector independent of any effects of the optical feedback resolution.

b. Optical Encoder Linkage Loading – At steady-state idle, the feedback force from the optical encoder linkage spring in the linear mask systems would be sufficient to overcome friction on the metering valve actuator and slew the valve open. The decrease solenoid would have to be cycled 45 times per second as shown in Figure 21 just to keep fuel flow constant. This high rate of cycling would reduce the operational life of the solenoid, therefore Hamilton Standard was requested to reduce the spring force during the final design effort.

c. Optical Position Feedback Resolution – Simulation analysis showed that the .051 mm (.002 inch) resolution of the optical position feedback is acceptable for a prototype unit. The resolution would cause some fuel flow limit cycling and spiking up to 22.7 kilograms per hour (±50 pounds per hour) but would cause no undesirable effects on engine operation during testing. The high frequency of the fuel flow spikes keeps the engine low rotor speed and turbine temperature variations small as shown in Figure 22. The turbine temperature variations were reviewed by the turbine group at Pratt & Whitney Aircraft and were judged acceptable. The .051 mm (.002 inch) resolution results in 12 solenoid cycles per second in steady-state – as compared to 10 cycles per second with a 12-bit resolution.

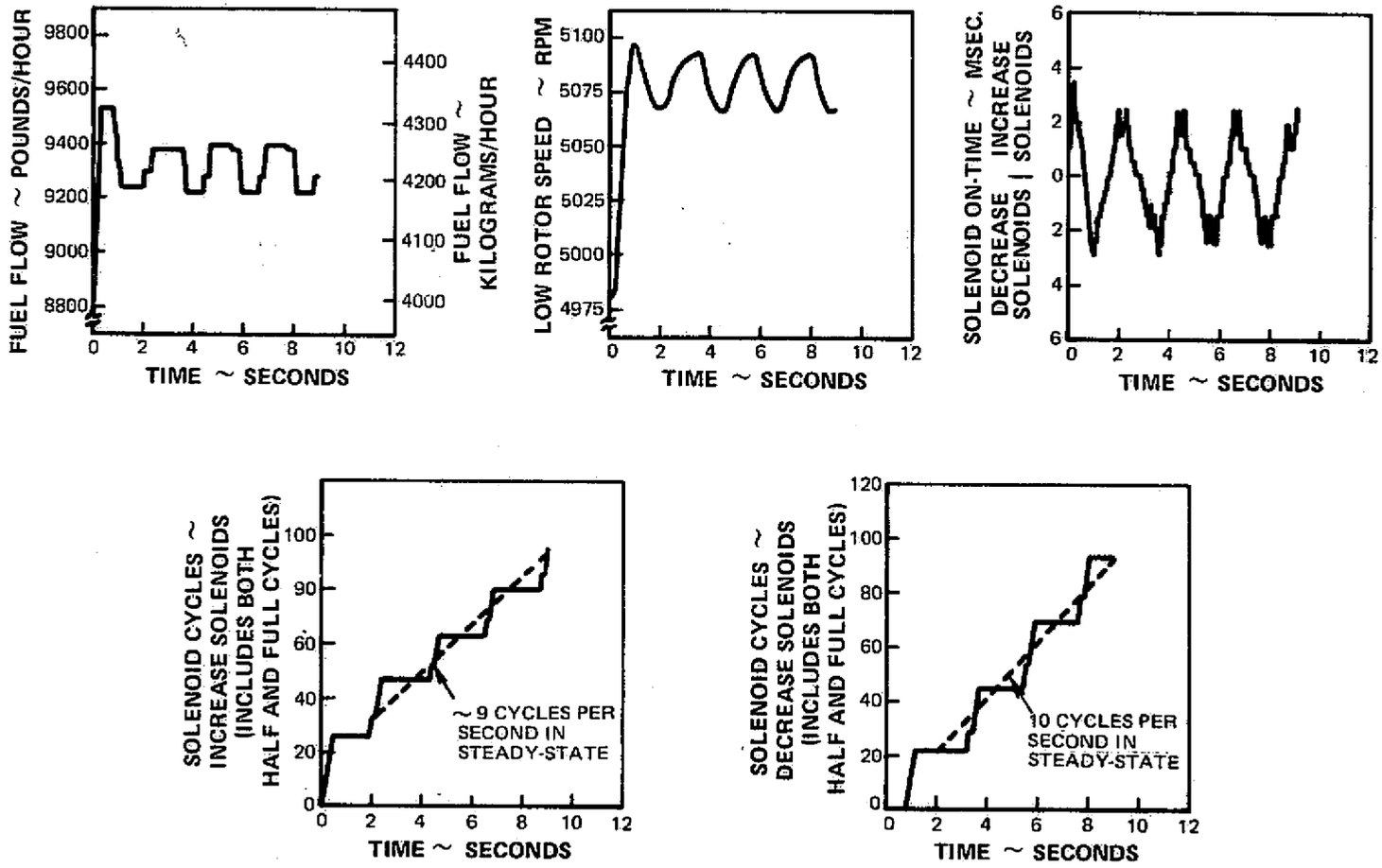

Figure 19 Small Power Lever Step and Steady-State Operation at Sea Level Static, High Power with the Two-Solenoid Configuration without Adaptive Logic

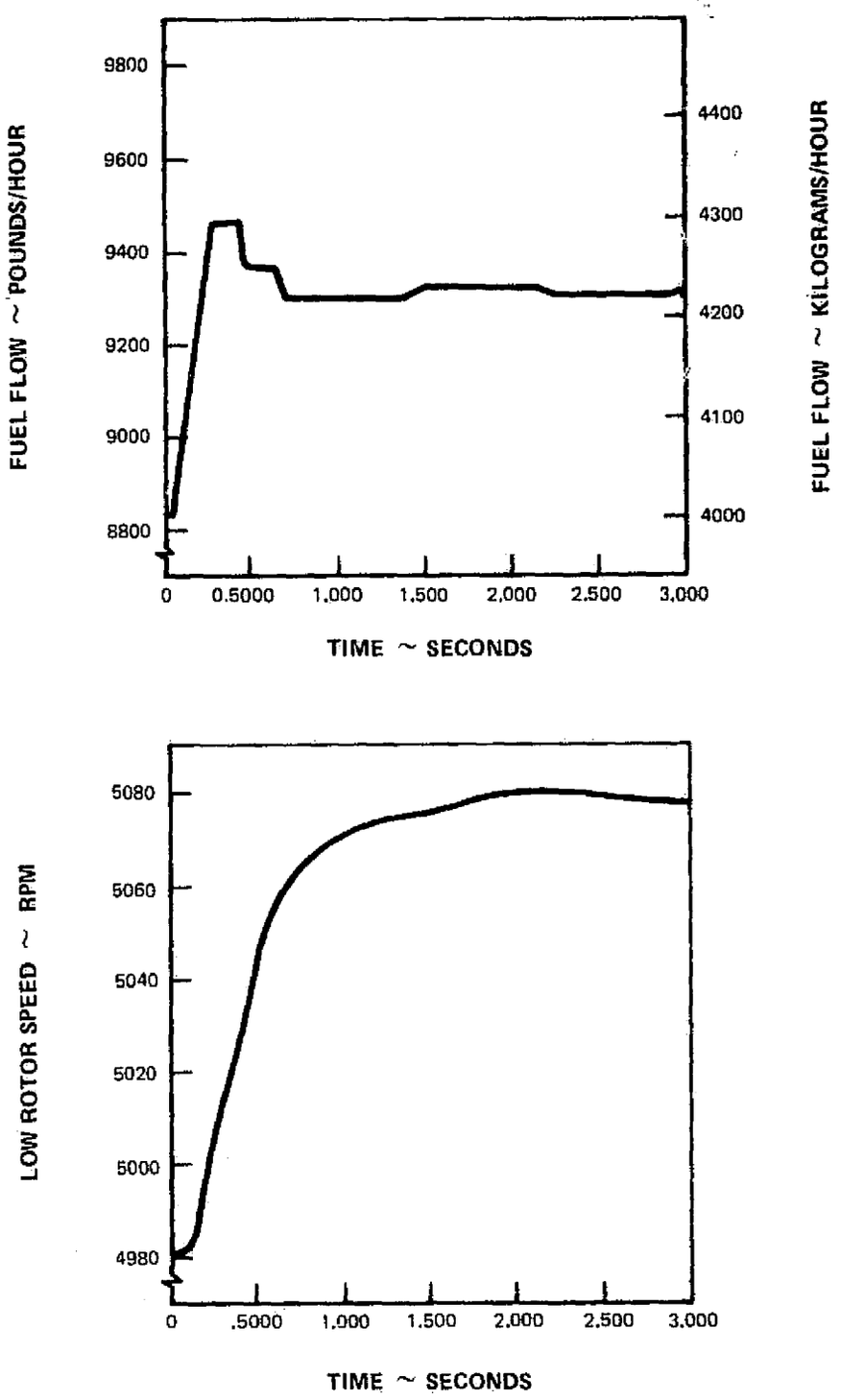

Figure 20 Response of the Two-Solenoid Digital Effector with 12-bit Position Feedback Resolution to Small Power Lever Step at Sea Level Static, High Power

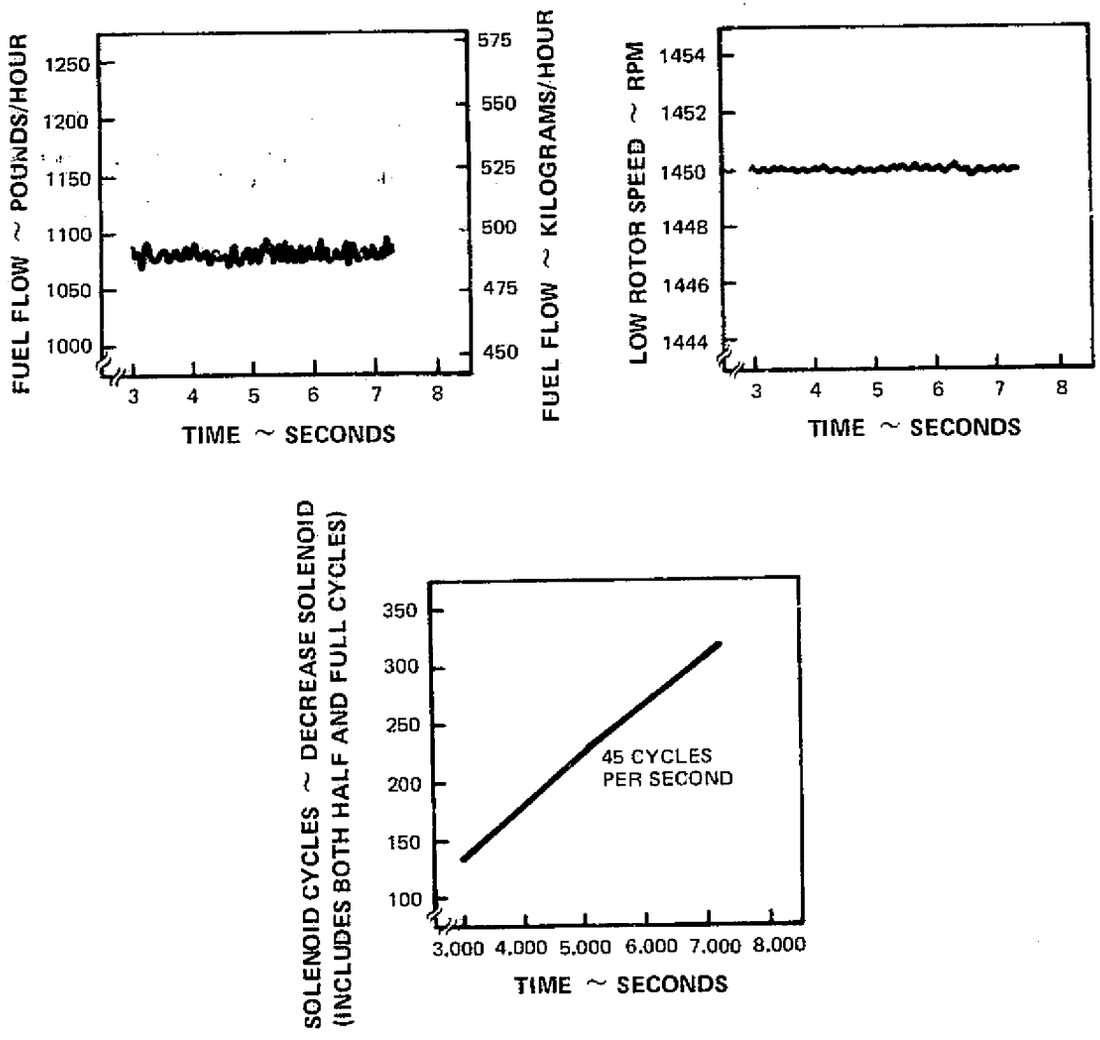

Figure 21 Steady-State Cycling at Idle Due to Optical Encoder Linkage Loading

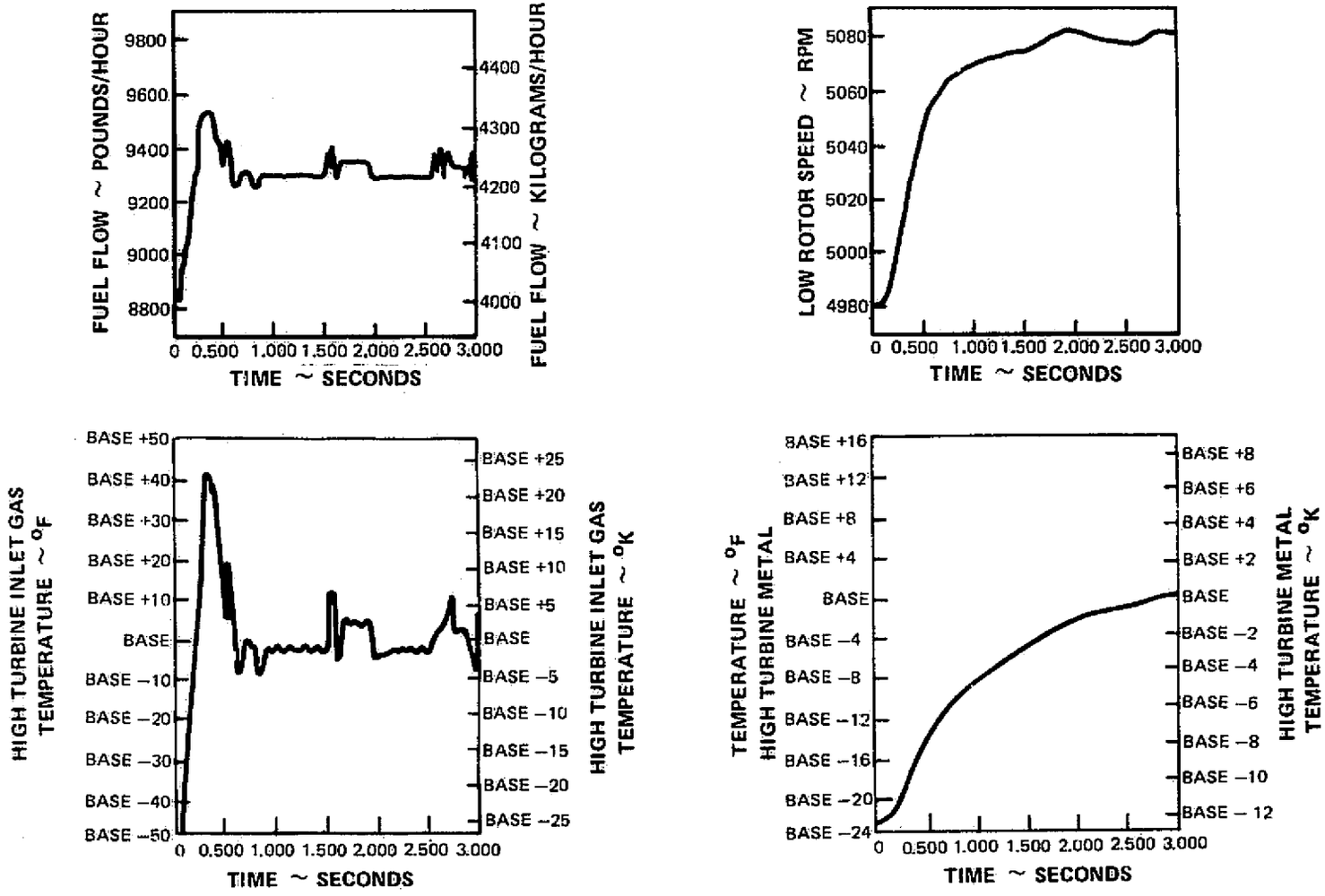

Figure 22 Response of Two-Solenoid Configuration with the Original Adaptive Logic and .002 Inch Position Feedback Resolution to a Small Power Lever Step at Sea Level Static, High Power

d. Failure Analysis of the Two-Solenoid Configuration – A solenoid failure could cause a fuel flow change and would always result in the loss of capability to move the fuel valve in one direction. For example, a solenoid failing open would cause the fuel valve to move in the corresponding direction. The electronic control would respond to the error between requested and measured fuel flow by opening the opposite solenoid for a portion of the computer cycle, slowing down the fuel flow rate of change. As the fuel flow error increases, the good solenoid stays on longer and will eventually be continuously energized, halting fuel valve motion. Fuel flow cannot be restored to the initial steady-state level because the solenoid which failed open prevents the fuel valve from moving in the required direction. A summary of the failure consequences of the two-solenoid configuration is shown in Table 12.

A solenoid failing closed would have a small or no effect on steady-state operation, except at idle where a failure of the decrease solenoid would cause fuel flow to increase until the spring loading is insufficient to overcome friction.

2. Review of Final Design

During the final design effort (Task 3), two redundant solenoids were added to improve operational reliability and to provide additional engine protection during testing. The sector-mask optical encoder chosen for final design provides an acceptable level of feedback force on the metering valve. The dynamic simulation was updated to reflect these changes.

a. Digital Effector: Four-Solenoid Configuration – Dynamic analysis of the four-solenoid configuration predicts response and stability better than the two-solenoid configuration. The solenoids in the four-solenoid configuration will be adjusted to slew only one half of the full stroke to maintain the same flow gain as the two-solenoid configuration. A small power lever transient and steady-state at high power with the four-solenoid scheme is shown in Figure 23. The shorter solenoid stroke to full open causes a faster transition to maximum fuel valve velocity. This permits less frequent control actuation than the two-solenoid, full-stroke configuration because the same solenoid on-time provides increased valve translation. The simulation predicts 2 solenoid cycles per second for the four-solenoid scheme with the revised adaptive logic as shown in Figure 23. The two-solenoid scheme would cycle 4 times per second with the same adaptive logic as shown in Figure 18.

b. Optical Encoder Linkage Loading – Solenoid cycling at idle has been greatly reduced by reducing the loading from the optical encoder feedback spring. The spring force will now be less than one-half of the actuator friction, therefore it is no longer necessary to cycle the decrease solenoid at steady-state idle. A small power level step and steady-state at idle (Figure 24) shows good steady-state stability and less than 2 solenoid cycles per second. The slow transient response is a result of the dynamic compensation in the electronic control not being optimized for low power operation.

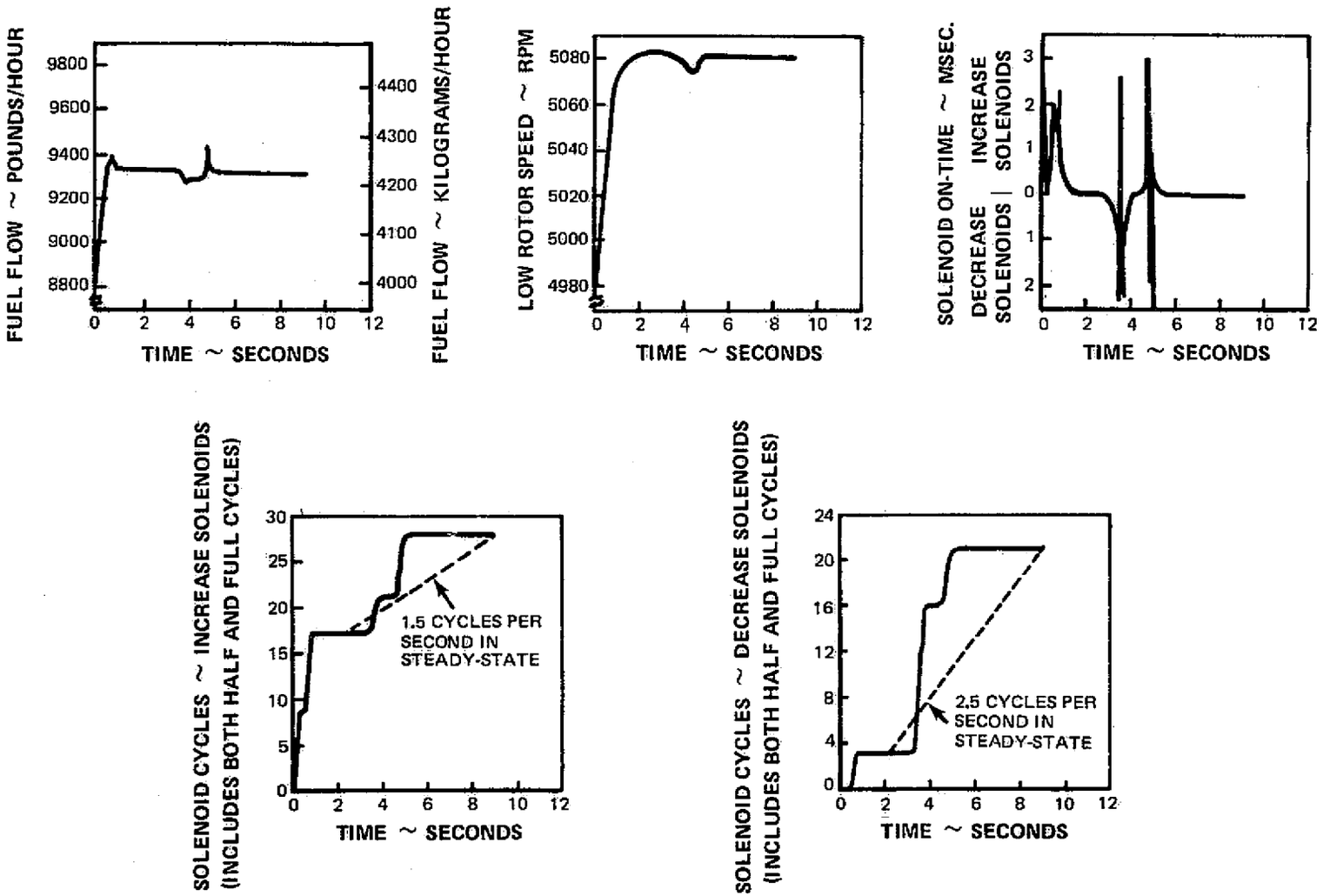

Figure 23 Small Power Lever Step and Steady-State Operation at Sea Level Static, High Power with the Four-Solenoid Configuration

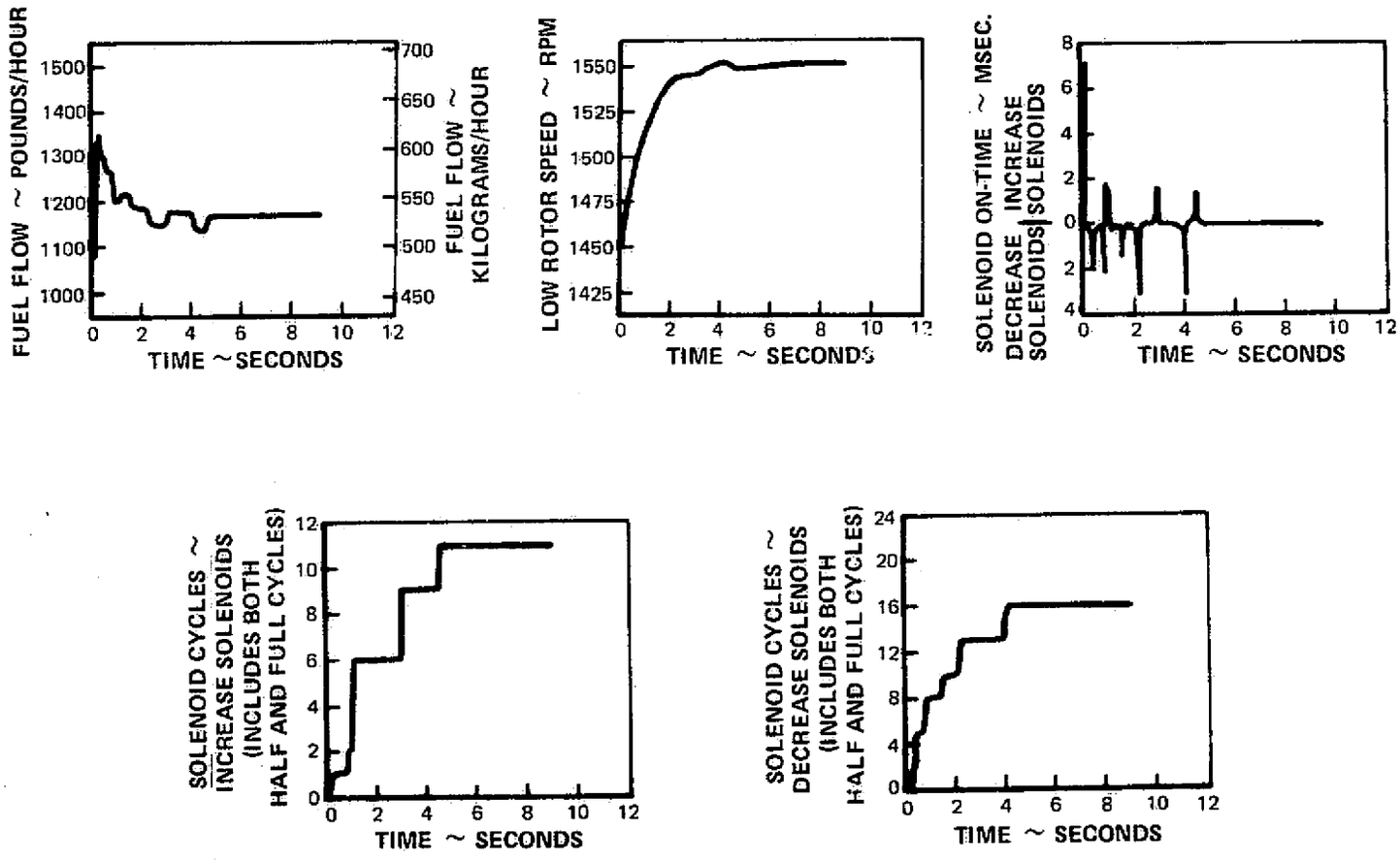

Figure 24 Small Power Lever Step and Steady-State Operation at Idle with the Four-Solenoid Configuration and with Reduced Loading from the Optical Encoder

c. Failure Analysis of the Four-Solenoid Configuration – The four-solenoid configuration will eliminate all undesirable consequences of any single solenoid failure because the two solenoids on the opposite side can override the failed solenoid. A solenoid failing open would cause a fuel flow change which is quickly overridden by the electronic control sensing an error between requested and measured fuel flow and consequently energizing both solenoids on the opposite side. A steady-state limit cycle would result as these two solenoids stay open approximately half the time. This failure mode is acceptable because the rotor speed variation and turbine temperature variations are small. The turbine temperature variations have been reviewed by the turbine group at Pratt & Whitney Aircraft and judged accpetable. After a solenoid fails open, fuel flow could still be varied in either direction although the rate limit in one direction would be lowered. Data from the simulation showing one increase solenoid failing open at high power is shown in Figure 25.

A solenoid failing closed would have little or no effect on steady-state operation. The fuel flow rate limit would be halved in one direction when a solenoid fails closed.

A summary of the failure analysis of the four-solenoid scheme is shown in Table 13. No undesirable failure consequences would result from a single solenoid failure.

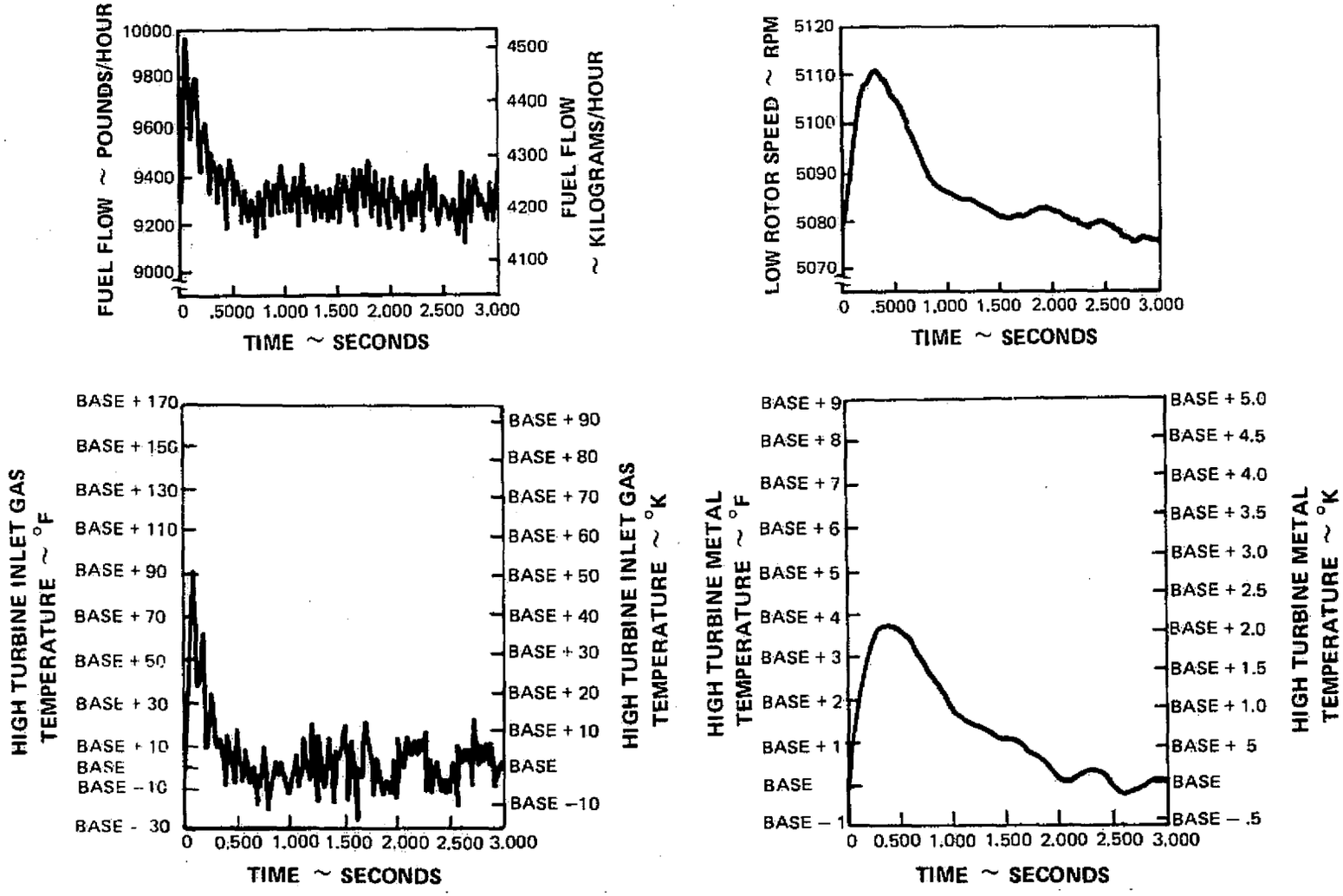

Figure 25 Response Due to One Increase Solenoid Failing Open at Sea Level Static, High Power

V. CONCLUSIONS

A program has been conducted to analyze and design digital output interface devices for gas turbine electronic controls. The objective of the program was to select a digital output interface device which has the potential for high reliability and low-cost maintainability in an aircraft gas turbine electronic control. The objective was met through a trade study to evaluate twenty-one digital output interface schemes and through the design of the best scheme based on the criteria of reliability, performance, life cycle cost and sampling requirements.

The trade study concluded that a digital effector with optical position feedback and adaptive logic in the software has potential reliability and cost advantages over more conventional digital output interface approaches. Torque motor and stepper motor DOI schemes would also provide adequate performance, but would be more expensive and less reliable than a digital effector. An optical position sensor has potential reliability and cost advantages over potentiometers, resolvers, and linear variable differential transformers (LVDT).

A prototype digital effector with optical position feedback and adaptive logic in the software was designed to operate the fuel metering valve of a gas turbine full authority electronic controller. The design of the digital effector includes two redundant solenoids to provide fail-safe protection during development testing.

TABLE 1
DIGITAL OUTPUT INTERFACE DEVICES COMPONENT DATA

COMPONENT	COST	WEIGHT kilograms(pounds)	ACCURACY	RELIABILITY (Failures per million hours)
Torque Motor and Drive Circuit	$455	.385(.85)	Gain ± 10% Hysteresis ± 2%	9.2
Stepper Motor, Gear Train, and Drive Circuit	$575	.227(.5)	Gain ±1% Hysteresis = 0 Granularity ± .2%	16.5
Digital Effector and Drive Circuit	$200	.317(.7)	Controlled by Processor Logic as required	5.5
Resolver	$180	.113(.25)	*	2.5
Linear Variable Differential Transformer (LVDT)	$200	.136(.3)	± 1.5%	5.0
Rate Sensor	$160	.109(.24)	± 15%	5.0
Optical Position Sensor	$150	.113(.25)	±.1%	2.5
Analog-to-Digital Converter (12 bit)	$150	.091(.2)	± .16%	9.7
Digital-to-Analog Converter (8 bit)	$ 40	.023(.05)	± .8%	3.0
Resolver-to-Digital Converter (12 bit)	$100	.045(.1)	± .00524 radians (± 18 minutes)	7.6
Rate Sensor Interface	$ 35	.014(.03)	± .25%	1.3
Optical Interface	$ 50	.045(.1)	Digital Absolute	3.0
Analog Integrator	$ 25	.014(.03)	± .15%	1.0
Resolver-to-Direct Current (D.C.) Converter	$100	.045(.1)	± .00524 radians (± 18 minutes)	5.8

*± .000873 radians (± 3 minutes) accuracy
± .0000157 radians/°K (± 3 minutes/100°F) temperature variation

TABLE 2

RELIABILITY OF THE DIGITAL OUTPUT INTERFACE SCHEMES

DOI SCHEME NUMBER	PARTS COUNT RELIABILITY, failures per million hours	OPERATIONAL RELIABILITY, failures per million hours
1 with resolver feedback	22.3	12.2
1 with LVDT[(a)] feedback	26.9	12.2
1 with optical feedback	17.7	12.2
2 with resolver feedback	20.0	20.0
2 with LVDT[(a)] feedback	17.2	17.2
3	12.2	12.2
4	26.9	12.2
5	18.5	18.5
6	Same as Scheme 1	
7	27.9	27.9
8	18.5	12.2
9	Same as Scheme 3	
10 with resolver feedback	24.8	16.5
10 with LVDT[(a)] feedback	30.2	16.5
10 with optical feedback	27.0	16.5
11	31.2	16.5
12	Same as Scheme 10	
13	16.5	16.5
14	31.2	31.2
15 with resolver feedback	24.8	24.8
15 with LVDT[(a)] feedback	30.2	30.2
15 with optical feedback	27.0	27.0
16 with resolver feedback	15.6	5.5
16 with LVDT[(a)] feedback	20.2	5.5
16 with optical feedback	11.0	5.5
17	5.5	5.5
18	20.2	5.5
19	Same as Scheme 16	
20	Same as Scheme 18	
21	Same as Scheme 17	

(a) Linear Variable Differential Transformer

TABLE 3

COST*, WEIGHT, MAINTENANCE AND LIFE CYCLE COST OF THE DIGITAL OUTPUT INTERFACE SCHEMES

SCHEME NUMBER & TYPE OF FEEDBACK	INITIAL COST - $ (1)	WEIGHT KILOGRAMS (POUNDS) (2)	RELIABILITY FAILURES MILLION HOURS (3)	MAINT. FAILURES $/MILLION HOURS (4)	MAINT. MATERIAL COST - $ (5)	FAILURES 50,000 HOURS (6)	MAINT. LABOR -$- (7)	PROCUREMENT COST -$- (8)	WEIGHT FACTOR -$- (9)	MAINT. COST -$- (10)	TOTAL -$- (11)
1 - resolver	775	0.57 (1.25)	22.3	5,516	275	1.115	142	969	167	417	1,553
1 - LVDT**	845	0.63 (1.4)	26.9	6,761	338	1.345	171	1,056	188	509	1,753
1 - optical	695	0.57 (1.25)	17.7	4,831	242	0.885	112	869	167	354	1,390
2 - resolver	775	0.57 (1.25)	20.0	5,336	267	1.0	127	969	167	394	1,530
2 - LVDT**	695	0.54 (1.2)	17.2	5,306	265	0.86	109	869	161	374	1,404
3	495	0.41 (0.9)	12.2	4,306	215	0.61	77	619	121	292	1,032
4	805	0.61 (1.34)	26.9	6,561	328	1.345	171	1,006	180	499	1,685
5	690	0.53 (1.17)	18.5	5,106	255	0.925	117	862	157	372	1,391
6				same as Scheme No. 1							
7	830	0.62 (1.37)	27.9	6,586	329	1.395	177	1,037	184	506	1,727
8				same as Scheme No. 5							
9				same as Scheme No. 3							
10 - resolver	885	0.38 (0.85)	24.8	10,517	526	1.24	157	1,069	114	683	1,866
10 - LVDT**	925	0.45 (1.0)	30.2	11,942	597	1.51	192	1,156	134	789	2,079
10 - optical	775	0.38 (0.85)	27.0	10,012	501	1.1	140	969	114	641	1,724
11	885	0.43 (0.94)	31.2	11,742	587	1.56	198	1,106	126	785	2,017
12				same as Scheme No. 10							
13	575	0.23 (0.5)	16.5	9,487	474	0.825	105	719	67	579	1,365
14				same as Scheme No. 11							
15				same as Scheme No. 10							
16 - resolver	480	0.48 (1.05)	15.6	2,310	116	0.78	99	600	141	215	956
16 - LVDT**	550	0.54 (1.2)	20.2	3,550	177	1.01	128	687	161	305	1,153
16 - optical	400	0.48 (1.05)	11.0	1,675	81	0.55	70	500	141	151	792
17	200	0.32 (0.7)	5.5	1,100	55	0.275	35	250	94	90	434
18	510	0.52 (1.14)	20.2	3,355	168	1.01	128	637	153	296	1,086
19				same as Scheme No. 16							
20				same as Scheme No. 18							
21				same as Scheme No. 17							

*1975 $
**Linear Variable Differential Transformer

Column 1 – Initial cost, sum of the component costs for each scheme.
Column 2 – Weight, sum of the component weights
Column 3 – Reliability, sum of the component rates
Column 4 – Sum of the component (cost X reliability), indication of maintenance material cost per million hours
Column 5 – Maintenance material cost for the assumed life of 50,000 hours
Column 6 – Failures that can be expected in 50,000 hours
Column 7 – Studies have predicted that the labor cost per repair of an electronic control will be $127 (assumes rate of $12.50/hour) - maintenance labor = (Failures in 50,000 hours) X 127
Column 8 – Procurement cost = Initial Cost (Column 1) X 1.25, 25% added as an arbitrary indication of spare control requirement.
Column 9 – Weight Factor, cost to fly X kilograms for 50,000 hours. Requires 0.4 kilograms JP4 to fly 1 kilogram dry weight for a 4848 kilometer (3000 mile) mission assume average speed of 257 meters per second (575 miles per hour) and JP4 @ $0.0519 per liter, cost to fly 1 kilogram of dry weight for 50,000 hours = $295.50
Column 10 – Maintenance Cost = Material (Column 5) + Labor (Column 7)
Column 11 – Total Life Cycle Cost - Columns 8 + 9 + 10

TABLE 4

PERFORMANCE EVALUATION OF THE DIGITAL OUTPUT INTERFACE SCHEMES

SCHEME NUMBER & TYPE OF FEEDBACK	TRANSIENT RESPONSE AT HIGH POWER W.F.* = 1			STEADY-STATE ACCURACY: CLOSED LOOP CONTROL W.F.* = 2			STEADY-STATE ACCURACY: OPEN LOOP CONTROL W.F.* = 2						STEADY-STATE STABILITY W. F. * = 2			TOTAL PERFORMANCE RANK
							Fuel Flow Error									
	Time to 90% Requested N1** Speed Change, Seconds	Rank	Total	N1** Speed Error ± RPM	Rank	Total	Low Power Kg/hr. (lbs./hr.)		High Power Kg/hr. (lbs./hr.)		Rank	Total	N1** Speed Limit Cycle ±RPM	Rank	Total	
1. Resolver	.93-1.09	2	2	0	1	2	21	(47)	64	(141)	2	4	1.6-2.3	2	4	12
1. LVDT	.93-1.09	2	2	0	1	2	44	(96)	131	(288)	4	8	1.6-2.3	2	4	16
1. Optical	.93-1.09	2	2	0	1	2	19	(41)	56	(123)	2	4	1.6-2.3	2	4	12
2. Resolver	.94-1.05	2	2	0	1	2	30	(66)	90	(198)	3	6	0-.7	1	2	12
2. LVDT	.94-1.05	2	2	0	1	2	48	(106)	144	(318)	4	8	0-.7	1	2	14
3	.88-1.04	2	2	0	1	2	205	(452)	615	(1356)	4+	8+	1.2-1.6	1	2	14+
4	.96-1.08	2	2	3.4	2	4	–	– –	–	– –	4+	8+	.5-2.3	1	2	16+
5	.98-1.10	2	2	8.7	2	4	–	– –	–	– –	4+	8+	1.8	2	4	18+
6. Resolver	.96-1.10	2	2	172.0	4+	8+	17	(37)	93	(205)	3	6	2.2	2	4	20+
6. LVDT	.96-1.10	2	2	172.0	4+	8+	42	(92)	147	(324)	4	8	2.2	2	4	22+
6. Optical	.96-1.10	2	2	172.0	4+	8+	13	(29)	88	(193)	3	6	2.2	2	4	20+
7	.97-1.09	2	2	17.8	3	6	–	– –	–	– –	4+	8+	2.1-4.8	2	4	20+
8	.88-1.0	2	2	122.0	4+	8+	–	– –	–	– –	4+	8+	.4-1.4	1	2	20+
9	.96-1.10	2	2	172.0	4+	8+	–	– –	–	– –	4+	8+	2.2	2	4	22+
10. Resolver	.82-.86	1	1	0	1	2	14	(30)	41	(90)	1	2	1.9	2	4	9
10. LVDT	.82-.86	1	1	0	1	2	40	(89)	121	(267)	4	8	1.9	2	4	15
10. Optical	.82-.86	1	1	0	1	2	9	(19)	26	(57)	1	2	1.9	2	4	9
11	.96-1.38	4	4	3.4	2	4	–	– –	–	– –	4+	8+	7.0	4	8	24+
12. Resolver	.95-1.35	4	4	73.0	4+	8+	12	(27)	49	(109)	1	2	.3	1	2	16+
12. LVDT	.95-1.35	4	4	73.0	4+	8+	40	(88)	124	(273)	4	8	.3	1	2	22+
12. Optical	.95-1.35	4	4	73.0	4+	8+	6	(14)	39	(85)	1	2	.3	1	2	16+
13	.95-1.35	4	4	73.0	4+	8+	–	– –	–	– –	4+	8+	.3	1	2	22+
14	1.09-1.45	4	4	3.4	2	4	–	– –	–	– –	4+	8+	6.1	4	8	24+
15. Resolver	1.03-1.11	2	2	21.0	3	6	–	– –	–	– –	4+	8+	1.2	1	2	18+
15. LVDT	.94-1.20	3	3	38.0	4	8	–	– –	–	– –	4+	8+	1.2	1	2	21+
15. Optical	1.06-1.08	2	2	20.0	3	6	–	– –	–	– –	4+	8+	1.2	1	2	18+
16. Resolver	.89-1.09	2	2	0	1	2	11	(24)	33	(72)	1	2	2.3-4.2	2	4	10
16. LVDT	.89-1.09	2	2	0	1	2	40	(87)	118	(261)	4	8	2.3-4.2	2	4	16
16. Optical	.89-1.09	2	2	0	1	2	4	(8)	11	(24)	1	2	2.3-4.2	2	4	10
18	.92-1.06	2	2	3.4	2	4	–	– –	–	– –	4+	8+	.9-2.1	1	2	16+
19. Resolver	.73-1.07	3	3	5.3	2	4	11	(24)	33	(72)	1	2	1.0	1	2	11
19. LVDT	.73-1.07	3	3	5.3	2	4	40	(87)	118	(261)	4	8	1.0	1	2	17
19. Optical	.73-1.07	3	3	5.3	2	4	4	(8)	11	(24)	1	2	1.0	1	2	11
20	.60-1.37	4	4	3.4	2	4	–	– –	–	– –	4+	8+	1.6	1	2	18+
21	.56-2.10	4	4	136	4+	8+	–	– –	–	– –	4+	8+	0.6	1	2	22+

* W. F. = Weighting Factor

** N1 = Low Rotor Speed

TABLE 5
SAMPLING TIME LIMITATIONS

SCHEME NO.	CLOSED LOOP CONTROL, Milliseconds	OPEN LOOP CONTROL, Milliseconds
1 with Resolver Feedback	45	15
1 with LVDT[a] Feedback	45	15
1 with Optical Feedback	45	15
2 with Resolver Feedback	120	120 (b)
2 with LVDT Feedback	120	120 (b)
3	90	90 (b)
4	45	– –
5	45	– –
6 with Resolver Feedback	120	30
6 with LVDT[a] Feedback	120	30
6 with Optical Feedback	120	30
7	45	– –
8	105	– –
9	120	– –
10 with Resolver Feedback	45	30
10 with LVDT[a] Feedback	45	30
10 with Optical Feedback	45	30
11	15	– –
12 with Resolver Feedback	90	30
12 with LVDT[a] Feedback	90	30
12 with Optical Feedback	90	30
13	90	– –
14	60	– –
15 with Resolver Feedback	45	– –
15 with LVDT[a] Feedback	45	– –
15 with Optical Feedback	45	– –
16 with Resolver Feedback	60	15
16 with LVDT[a] Feedback	60	15
16 with Optical Feedback	60	15
18	45	– –
19 with Resolver Feedback	30	15
19 with LVDT[a] Feedback	30	15
19 with Optical Feedback	30	15
20	105	– –
21	105	– –

(a) Linear Variable Differential Transformer

(b) Sampling limit for open loop control was not investigated beyond the limit established for closed loop control

TABLE 6

PERFORMANCE EVALUATION OF THE MOST PROMISING DIGITAL OUTPUT INTERFACE SCHEMES AT SEA LEVEL STATIC

SCHEME NUMBER	TRANSIENT RESPONSE AT HIGH POWER Weight Factor = 1			STEADY-STATE ACCURACY CLOSED LOOP CONTROL Weight Factor = 2			STEADY-STATE ACCURACY OPEN LOOP CONTROL Wt. Factor = 2				STEADY-STATE STABILITY Wt. Factor = 2			TOTAL PERFORMANCE RANKING
	Time to 90% of Requested Low Rotor Speed Change, Seconds	Rank	Total	Low Rotor Speed Error, ± RPM	Rank	Total	Fuel Flow Error: Low Power Kg/hr (lbs/hr)	Fuel Flow Error: High Power Kg/hr (lbs/hr)	Rank	Total	N1 Speed Limit Cycle ± RPM	Rank	Total	
1. Optical	.93 – 1.09	2	2	0	1	2	19 (41)	56 (123)	3	6	1.6 – 2.3	3	6	16
2. Resolver	.94 – 1.05	2	2	0	1	2	30 (66)	90 (198)	4	8	0–.7	1	2	14
10. Optical	.82 – .86	1	1	0	1	2	9 (19)	26 (57)	2	4	1.9	3	6	13
16. Optical	.89 – 1.09	2	2	0	1	2	4 (8)	11 (24)	1	2	2.3 – 4.2	4	8	14
19. Optical	.73 – 1.07	2	2	5.3	4	8	4 (8)	11 (24)	1	2	1.0	2	4	16

TABLE 7
PERFORMANCE EVALUATION OF THE MOST PROMISING DIGITAL OUTPUT INTERFACE SCHEMES AT ALTITUDE CRUISE

SCHEME NUMBER	TRANSIENT RESPONSE AT HIGH POWER Wt. Factor = 1			STEADY-STATE ACCURACY CLOSED LOOP CONTROL Weight Factor = 2			STEADY-STATE ACCURACY OPEN LOOP CONTROL Wt. Factor = 2				STEADY-STATE STABILITY Wt. Factor = 2			TOTAL PERFORMANCE RANKING
	Time to 80% of Requested N1 Change, Sec.	Rank	Total	N1 Speed Error ±RPM	Rank	Total	Fuel Flow Error Low Power Kg./hr. (lbs./hr.)	Fuel Flow Error High Power Kg./hr. (lbs./hr.)	Rank	Total	N1 Speed Limit Cycle ±RPM	Rank	Total	
1. Optical	1.18-1.32	2	2	0	1	2	13 (29)	42 (92)	3	6	1.8-3.7	4	8	18
2. Resolver	1.22-1.26	1	1	0	1	2	21 (47)	67 (148)	4	8	.5-1.6	1	2	13
10. Optical	1.26-1.30	1	1	0	1	2	6 (13)	20 (43)	2	4	2.7	4	8	15
16. Optical	1.19-1.31	2	2	0	1	2	3 (6)	8 (18)	1	2	1.7-3.0	3	6	12
19. Optical	1.01-1.60	4	4	10.3	4	8	3 (6)	8 (18)	1	2	.7-3.5	3	6	20

TABLE 8
FINAL PERFORMANCE EVALUATION OF THE MOST PROMISING DIGITAL OUTPUT INTERFACE SCHEMES

SCHEME NUMBER	SEA LEVEL STATIC TOTAL PERFORMANCE RANKING(1)	ALTITUDE CRUISE TOTAL PERFORMANCE RANKING(2)	OVERALL PERFORMANCE RANKINGS	RANK
1 Optical	16	18	34	3
2 Resolver	14	13	27	1
10 Optical	13	15	28	2
16 Optical	14	12	26	1
19 Optical	16	20	36	4

(1) From Table 6
(2) From Table 7

TABLE 9

SAMPLING INTERVAL TIME EVALUATION OF THE MOST PROMISING DIGITAL OUTPUT INTERFACE SCHEMES

SCHEME NUMBER	MAXIMUM SAMPLING INTERVAL FOR ADEQUATE OPERATION WITH: CLOSED LOOP CONTROL (Milliseconds)	RANK	OPEN LOOP CONTROL (Milliseconds)	RANK	TOTAL	RANK
1. Optical	45	3	15	4	7	3
2. Resolver	120	1	120	1	2	1
10. Optical	45	3	30	3	6	3
16. Optical	60	3	15	4	7	3
19. Optical	30	4	15	4	8	4

TABLE 10
FINAL EVALUATION OF THE MOST PROMISING DIGITAL OUTPUT INTERFACE SCHEMES

Scheme Number	Performance (1) Weight Factor = 3		Sample Time (2) Weight Factor = 1		Reliability (3) Weight Factor = 3			Life Cycle Cost (3) Weight Factor = 2			Total
	Rank	Total	Rank	Total	Rate x 10^6	Rank	Total	LCC-$	Rank	Total	
1. Optical	3	9	3	3	17.7	3	9	1390	3	6	27
2. Resolver	1	3	1	1	20.0	3	9	1530	3	6	19(4)
10. Optical	2	6	3	3	22.0	4	12	1724	4	8	29
16. Optical	1	3	3	3	11.0	1	3	792	1	2	11
19. Optical	4	12	4	4	11.0	1	3	792	1	2	21

(1) From Table 8
(2) From Table 9
(3) From Table 3
(4) Evaluation based on parts count (MTBF) reliability only, operation reliability of Scheme 2 much lower than other schemes.

TABLE 11
COMPARISON OF GRAY AND BINARY CODES

GRAY					BINARY				DECIMAL
0	0	0	0	=	0	0	0	0	0
0	0	0	1		0	0	0	1	1
0	0	1	1		0	0	1	0	2
0	0	1	0		0	0	1	1	3
0	1	1	0		0	1	0	0	4
0	1	1	1		0	1	0	1	5
0	1	0	1		0	1	1	0	6
0	1	0	0		0	1	1	1	7
1	1	0	0		1	0	0	0	8
1	1	0	1		1	0	0	1	9
1	1	1	1		1	0	1	0	10
1	1	1	0		1	0	1	1	11
1	0	1	0		1	1	0	0	12
1	0	1	1		1	1	0	1	13

TABLE 12
SOLENOID FAILURE CONSEQUENCES: TWO-SOLENOID SCHEME

	IDLE POWER		TAKE-OFF POWER	
	INCREASE SOLENOID	DECREASE SOLENOID	INCREASE SOLENOID	DECREASE SOLENOID
Fails Closed	No effect on steady-state fuel flow. Cannot increase fuel flow.	Spring load will cause fuel valve to slew open. Resulting fuel flow will be between 770 and 1225 kilograms per hour (1700 and 2700 pounds per hour), depending on piston leakage. Cannot decrease fuel flow.	Small fuel flow decrease (23 kilograms per hour, 50 pounds per hour). Cannot increase fuel flow.	Small fuel flow increase (23 kilograms per hour, 50 pounds per hour). Cannot decrease fuel flow.
Fails Open	Electronic control will sense fuel flow error and open decrease solenoid. Results same as failing decrease solenoid closed. Cannot decrease fuel flow.	Fuel flow will decrease toward min. flow. Controller will sense error and open increase solenoid. Fuel flow recovers to -181 to 0 kilograms per hour (-400 to 0 pounds per hour) below original value, depending on leakage. Cannot increase fuel flow.	Fuel valve will slew open, controller will sense error and open the decrease solenoid. A 771 kilogram per hour (1700 pound per hour) fuel flow increase will result. Cannot decrease fuel flow.	Fuel valve will slew closed, electronic control will sense error and open the increase solenoid. A 680 kilogram per hour (1500 pound per hour) fuel flow decrease will result. Cannot increase fuel flow.

TABLE 13
SOLENOID FAILURE CONSEQUENCES: FOUR-SOLENOID SCHEME

	IDLE POWER		TAKE-OFF POWER	
	INCREASE SOLENOID	DECREASE SOLENOID	INCREASE SOLENOID	DECREASE SOLENOID
Fails Closed	No effect on steady-state.	No effect on steady-state.	No effect on steady-state.	No effect on steady-state.
Fails Open	Fuel valve will start opening, control will sense error and open the two decrease solenoids to drop fuel flow. An initial fuel flow increase of 496 kilograms per hour (225 pounds per hour) would result followed by a steady state limit cycle 27 kilograms per hour (60 pounds per hour) peak-to-peak at 13 hz. Negligible initial low rotor speed increase and negligible steady-state speed variation. Turbine temperature variation acceptable.	Fuel valve will start closing, control will sense error and open the two increase solenoids to raise fuel flow. An initial fuel flow decrease of 73 kilograms per hour (160 pounds per hour) would result followed by a steady state limit cycle 34 kilograms per hour (75 pounds per hour) peak-to-peak at 12 hz. Initial fuel flow drop is well above min. fuel-air flameout limit. Negligible initial low rotor speed decrease and negligible steady-state speed variation. Turbine temperature variation acceptable.	Fuel valve will start opening, control will sense error and open the two decrease solenoids to drop fuel flow. An initial fuel flow increase of 295 kilograms per hour (650 pounds per hour) would result followed by a steady-state limit cycle 113 kilograms per hour (250 pounds per hour) peak-to-peak at 12 hz. Initial 30 RPM low rotor speed increase. Steady-state low rotor speed variation negligible and turbine temperature variation acceptable.	Fuel valve will start closing, control will sense error and open the two increase solenoids to raise fuel flow. An initial fuel flow decrease of 295 kilograms per hour (650 pounds per hour) would result, followed by a steady-state limit cycle 113 kilograms per hour (250 pounds per hour) peak-to-peak at 13 hz. Initial 30 RPM low rotor speed decrease. Steady-state low rotor speed variation negligible and turbine temperature variation acceptable.

APPENDIX A

BLOCK DIAGRAMS OF DOI SCHEMES

LEGEND

D/A	—	Digital To Analog Converter
A/D	—	Analog To Digital Converter
T/M	—	Torque Motor
S/M	—	Stepper Motor
M.V.	—	Fuel Metering Valve
K	—	Gain
$\frac{K}{S}$	—	Integrator (Software or Hardware)
S	—	Rate

SCHEME 1

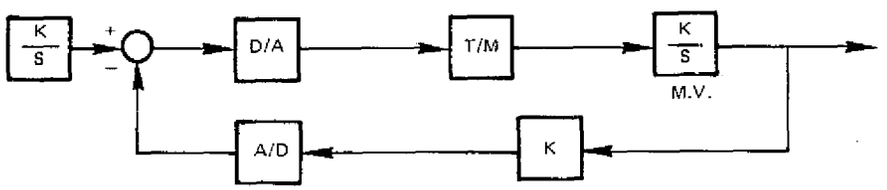

SCHEME 2

SCHEME 3

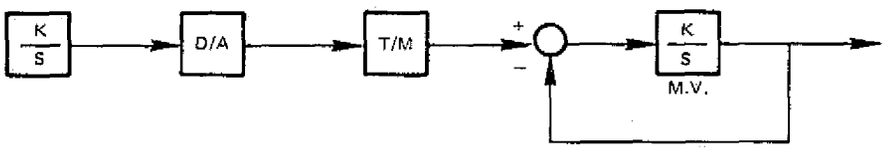

SCHEME 4

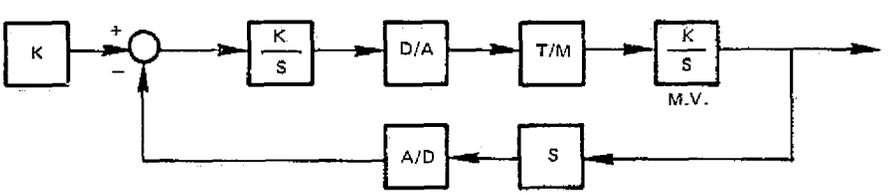

SCHEME 5

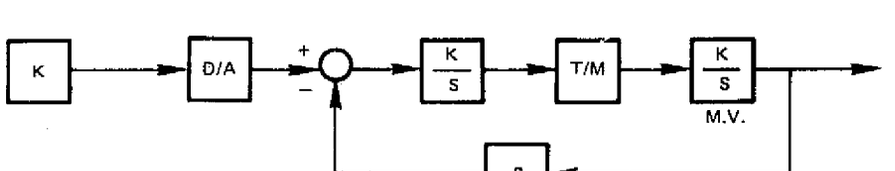

SCHEME 6

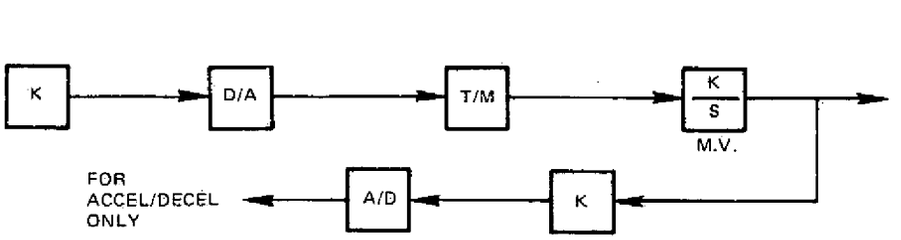

SCHEME 7

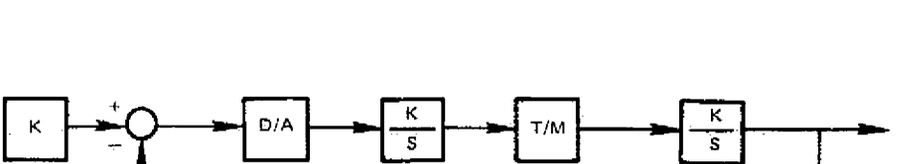

SCHEME 8

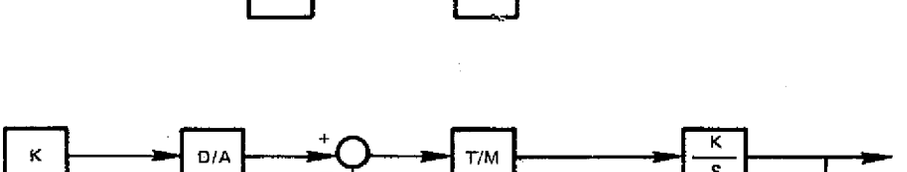

SCHEME 9

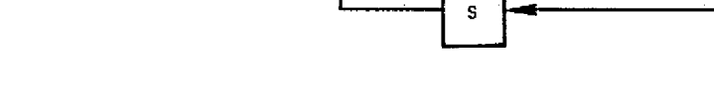

SCHEME 10

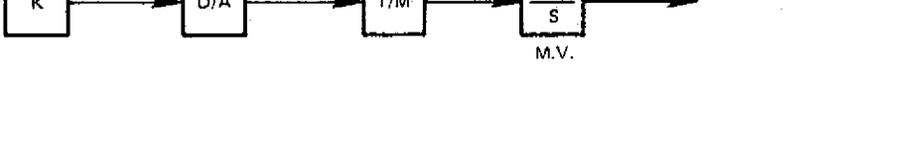

SCHEME 11

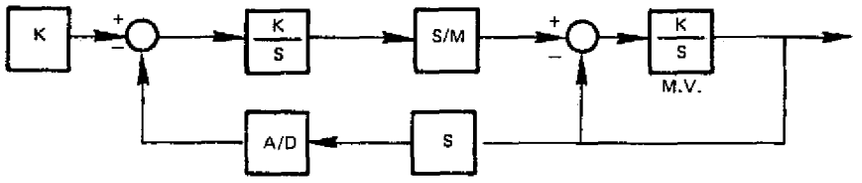

SCHEME 12

SCHEME 13

SCHEME 14

SCHEME 15

SCHEME 16

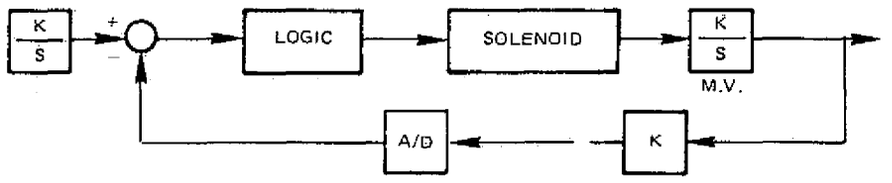

SCHEME 17

SCHEME 18

SCHEME 19

SCHEME 20

SCHEME 21

APPENDIX B

CALCULATION OF ADAPTIVE GAIN

SIMPLIFIED DIAGRAM OF METERING VALVE POSITION CONTROL LOOP

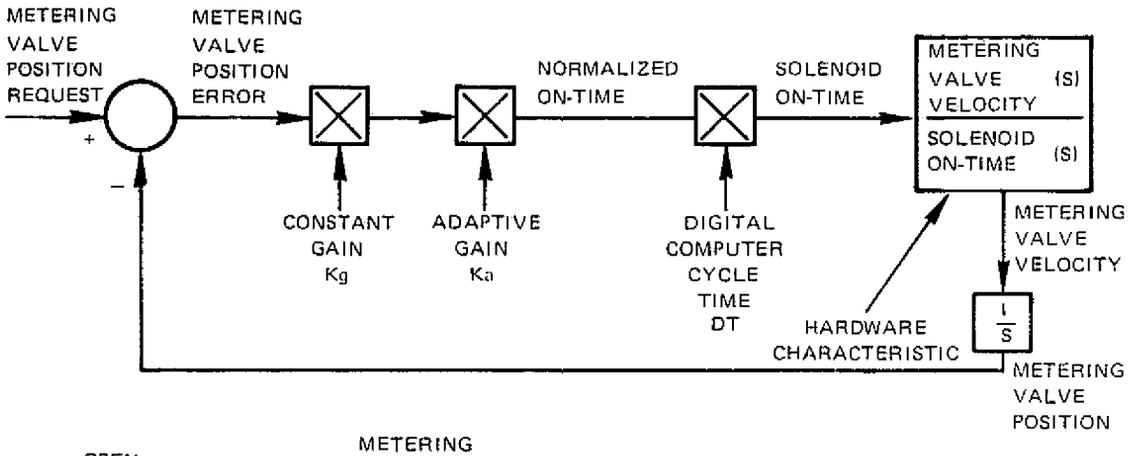

$$\text{(B1)}\quad \text{OPEN LOOP GAIN} = Kg * Ka * \frac{\text{METERING VALVE VELOCITY}}{\text{(SOLENOID ON TIME)}} * DT$$

$$\text{(B2)}\quad \text{METERING VALVE VELOCITY} = \left(\text{PRESENT POSITION} - \text{PAST POSITION}\right) / DT$$

$$\text{(B3)}\quad \text{OPEN LOOP GAIN} = Kg * Ka * \frac{\left(\text{PRESENT POSITION} - \text{PAST POSITION}\right) / DT}{\text{(SOLENOID ON TIME)}/DT}$$

$$\text{(B4)}\quad \text{OPEN LOOP GAIN} = Kg * Ka * \frac{\left(\text{PRESENT POSITION} - \text{PAST POSITION}\right) / DT}{\text{NORMALIZED ON TIME}}$$

SET: DESIRED GAIN = OPEN LOOP GAIN

$$\text{(B5)}\quad \text{DESIRED GAIN} = Kg * Ka * \frac{\left(\text{PRESENT POSITION} - \text{PAST POSITION}\right) / DT}{\text{NORMALIZED ON TIME}}$$

SOLVE FOR Ka:

$$\text{(B6)}\quad Ka = \frac{\text{DESIRED GAIN}}{Kg} * \frac{\text{NORMALIZED ON TIME}}{\left(\text{PRESENT POSITION} - \text{PAST POSITION}\right) / DT}$$